***Geostatistical Block-Support Simulation for Iron in Tailings: Addressing Non-Additivity***


by

Alibek Abilgazym

THESIS SUPERVISOR

Nasser Madani


Thesis submitted to the School of Mining and Geosciences of Nazarbayev University in Partial Fulfillment of the Requirements for the Degree of
**Bachelor of Science in Mining Engineering**

**Nazarbayev University**
**16.04.2025**

**ORIGINALITY STATEMENT**

I, Alibek Abilgazym, hereby declare that this submission is my work and to the best of my knowledge it contains no materials previously published or written by another person, or substantial proportions of material which have been accepted for the award of any other degree or diploma at Nazarbayev University or any other educational institution, except where due acknowledgement is made in the thesis.

Any contribution made to the research by others, with whom I have worked at NU or elsewhere, is explicitly acknowledged in the thesis.

I also declare that the intellectual content of this thesis is the product of my work, except to the extent that assistance from others in the project's design and conception or style, presentation, and linguistic expression is acknowledged.

Signed on 16.04.2025

## ABSTRACT

This study investigates the application of Sequential Gaussian Co-Simulation (SGCS) with block support to model the spatial distribution of iron (Fe) grade within a copper-gold mine tailings facility. The primary challenge addressed is the non-additive nature of iron grade, which limits the effectiveness of traditional interpolation methods that rely on linear averaging. Inaccurate modeling of such variables can lead to substantial errors in resource estimation, impacting both production planning and economic viability. To overcome this, SGCS was employed due to its capacity to incorporate secondary variables and better capture spatial variability and uncertainty. The block-support methodology was integrated to enhance the realism of the simulation by averaging sub-block realizations within larger blocks, thereby reducing interpolation error. However, block support can also suppress local extremes, which may lead to the underestimation of high values and the overestimation of low ones. In this study, density was estimated and used as a secondary variable for co-simulation due to its physical relevance and influence on Fe distribution. The simulations were conducted using Isatis.neo software, with validation performed through histogram analysis, swath plots, variogram reproduction, and cut-off tonnage curves. While the SGCS preserved spatial trends of the iron grade distribution and variogram structures effectively, the smoothing effect inherent to block support remained a limiting factor in capturing extreme values. Overall, the results demonstrate that SGCS with block support provides a robust approach for modeling non-additive variables in complex geological environments like tailings storage facilities. The findings contribute to improved geostatistical modeling approaches in resource estimation and highlight the importance of secondary variable selection, support size, and validation strategies.

**ACKNOWLEDGMENT**

I would like to express my gratitude to my supervisor, Professor Nasser Madani, someone whom I will always appreciate. I eventually succeeded in finishing my BSc thesis within the allocated time due to his guidance and encouragement. I appreciate it.

My family and my friends have been there for me no matter what during this research effort, and for that, I cannot thank them enough.

# TABLE OF CONTENTS

## LIST OF FIGURES

# LIST OF TABLES

# 1. INTRODUCTION

## 1.1 Background/Problem Definition

Geostatistics is a powerful analytical method used to interpret spatially distributed data. It integrates data with their physical coordinates and employs various interpolation techniques, including stochastic and deterministic methodologies, to estimate values in areas where direct sampling has not been conducted (ESRI, n.d.). Deterministic methods rely solely on measured data and mathematical calculations, producing results based only on the available dataset. However, the models estimated by using the deterministic methodologies often suffer from the smoothing effect. In other words, the lower values are overestimated, and the upper values are underestimated. In contrast, stochastic approaches incorporate statistical properties, enhancing the prediction model and improving the reliability of the resultant geospatial model (Brindha, Semiromi, Boumaiza, & Mukherjee, 2023). The geostatistical analysis is widely applied across various fields, including soil sciences, environmental studies, meteorology, and mining (ESRI, n.d..). In the mining industry, geostatistical analysis plays a fundamental role in resource estimation, which is a critical component at every stage of a mining project. Accurate resource estimation directly influences project feasibility, economic planning, decision-making, and engineering strategies. One of the primary objectives of resource estimation is to develop a geological model that represents the spatial distribution of key variables or characteristics within a deposit. This geological model provides valuable insights into parameters such as ore reserves, cut-off grade, and metal content. Based on these insights, engineering teams conduct further analyses and make strategic decisions about the future of the deposit (ESRI, n.d..). By integrating geostatistical techniques, mining operations can optimize extraction methods, processing strategies, and overall operational efficiency, leading to improved resource utilization and economic outcomes. Considering the latest global ecological trends, geostatistical modeling and estimation for tailings and waste dumps have become increasingly relevant. The rising importance of ecological values has led to a growing focus on sustainability in mining operations. The transition to green energy and eco-friendly environments will require vast amounts of natural resources (European Commission, 2020). Additionally, factors such as continuous population growth further increase the demand for mineral resources (Herrington, 2021). As a result, mining operations remain an essential component of future development. However, modern ecological requirements necessitate a commitment to sustainable development, which mandates minimizing the environmental and social impacts of mining and its production chain (Herrington, 2021). A key aspect of sustainable mining is the management of tailings and waste materials from both past and future mining operations. The mine tailings facilities have a severe negative impact on the local environment and human health. A high content of toxic elements, like lead and arsenic, and acidic content, which could be a result of the extraction of acidic elements like sulfur within the tailings, result in the drainage to the local waters and worsening the local soil. One effective strategy for tailings and waste management is re-mining, which addresses increasing production demands while ensuring economic viability and meeting ecological obligations, thereby reducing the environmental footprint (Blannin et al., 2023). Even though tailings and waste materials are byproducts of mineral extraction and processing (Bamigboye et al., 2021), they still contain significant amounts of valuable raw materials due to the lower efficiency of past processing methods and their previous lack of economic interest to the mining industry. Many tailings deposits hold critical raw materials (CRMs), including metals essential for modern technologies. With advancements in processing techniques, the recovery of these materials has become increasingly feasible. As a result, re-mining tailings presents an opportunity not only to meet the growing demand for these types of minerals but also to deal with the waste material (Blannin et al., 2023). Moreover, the re-mining of tailing storage facilities (TSFs) is advantageous compared to exploiting new deposits since they are more accessible and less energy-consuming for extracting and processing (Koucham et al., 2024). This approach enhances resource utilization while minimizing environmental impact, making it a sustainable strategy for managing mining waste. Consequently, tailings and waste facilities are gaining increased attention from mining companies worldwide. Given their potential for resource recovery and environmental sustainability, it is crucial to develop accurate resource estimation methods for tailings and waste dumps. Geostatistical modeling is essential for evaluating the economic feasibility of re-mining initiatives while ensuring adherence to modern environmental regulations. However, the geostatistical modeling of mine tailings is associated with multiple challenges.

- TSF Deposition Methods: The method of tailings formation and the location of spill points significantly influence the distribution of minerals within the tailings. This results in heterogeneity, complicating overall modeling and analysis.
- Chemical and Mineralogical Changes: Over time, tailings undergo chemical reactions due to oxidation, weathering, and leaching, altering their composition. While these changes may not directly impact grade distribution, they can significantly affect future reprocessing potential.

- Density Variations: Since most tailings are deposited as slurry, their particles can migrate within the deposit, leading to compaction, consolidation, and settlement of higher-density particles at the bottom layers.
- Non-Additivity of Interpolated Variables: Certain elements, such as iron and other metals, exhibit non-additive behavior, meaning their values cannot be directly averaged. To address this, advanced geostatistical approaches are required to mitigate the limitations associated with non-additivity.
- Data Limitations and Uncertainty: For precise TSF modeling, it is crucial to gather historical records on ore properties, processing methods, past topographies, spill point locations, and density measurements. However, gaps in historical data complicate the interpolation process, necessitating the use of simplified estimations to substitute for missing realistic data.

## 1.2 Objectives of the Thesis

### *1.2.1 Main Objectives*

● To develop a comprehensive geostatistical modeling framework for resource estimation within tailings storage facilities (TSFs) through the application of sequential Gaussian co-simulation (SGCS), with a particular focus on addressing challenges posed by non-additive variables such as iron grade.

### *1.2.2 Specific Objectives*

● To review and compare various geostatistical interpolation methods, including kriging and stochastic simulation techniques, based on insights from previous studies.

●To apply SGCS methodology to model the spatial distribution of iron grade in the Haveri TSF, incorporating block support and a secondary variable to improve accuracy.

●To validate the geostatistical model through statistical and spatial analysis techniques, including histogram comparison, variogram reproduction, and swath plot analysis.

## 1.3 Justification of the R&D

This study supports the development of more sustainable mining practices by improving the accuracy of resource estimation in mine tailings. By enhancing the reliability of modeling techniques for non-additive variables, the research contributes to the optimization of re-mining operations, promotes efficient resource utilization, and reduces the environmental footprint of mining activities. The outcomes of this research are particularly relevant as the industry shifts towards circular economy principles and critical raw material recovery.

## 1.4 Scope of Work

● **Literature Review:** Analyze prior research on interpolation methods used for modeling non-additive variables in mine tailings.

●**Secondary Variable Estimation:** Estimate the density of tailings material using a weighted average approach based on chemical composition data to be used as a secondary variable in the co-simulation process.

●**Geostatistical Modeling:** Apply the SGCS methodology to the Haveri TSF dataset, incorporating block support and co-simulation techniques to improve modeling accuracy.

● **Model Validation:** Assess the accuracy of the simulation outcomes by comparing them with the original sampling data using histogram analysis, variogram reproduction, and swath plot validation.

# 2. LITERATURE REVIEW

This chapter presents a comprehensive literature review of geostatistical methodologies applied to the modeling of non-additive variables in mining contexts. It focuses on grade modeling within mine tailing deposits, emphasizing findings from relevant case studies. Key topics include the challenges posed by non-additivity, the application of various interpolation techniques such as kriging and simulation, the role of support methodologies, and strategies for constructing accurate and reliable geospatial models of mine tailings.

## 2.1 Resource Estimation and Geostatistical Modeling

Resource estimation is a fundamental component of modern mining. Over recent decades, significant advancements in estimation techniques have enabled more effective handling and geologically interpreting spatially distributed, qualitative data and associated uncertainties (Rossi & Deutsch, 2014; The Australasian Institute of Mining and Metallurgy, 2014). Despite significant advancements in resource estimation and geostatistical methods, these processes cannot rely solely on software, as doing so may lead to implausible, inefficient, and potentially flawed financial and planning outcomes. It is important to conduct resource estimation under the supervision of a team of professionals in multiple spheres, like exploration, sampling, interpolation, geology, geo-modeling, and geostatistics, who will validate the estimation process and results (The Australasian Institute of Mining and Metallurgy, 2014). Resource estimation supports three key planning horizons: long-term, medium-term, and short-term. Long-term models represent the entire lifespan of a deposit and are typically updated every 1 to 3 years. Medium-term models are designed for planning activities within a time frame of 6 months to 1 year. Short-term models are updated daily or weekly to guide operational decisions and grade control during active mining operations (Rossi & Deutsch, 2014). Developing a reliable geological model is a crucial step in resource estimation. Therefore, accurate geostatistical modeling is essential for ensuring that resource estimates reflect the true spatial distribution of mineralization. This accuracy supports critical functions such as mine planning, production forecasting, process optimization, and environmental management. (The Australasian Institute of Mining and Metallurgy, 2014). Altogether, these factors impact the economic part of the mine project and play a critical role in determining the feasibility and progression of mining projects (Rossi & Deutsch, 2014). The accuracy of resource estimation outcomes depends heavily on factors such as the technical expertise of mine personnel, the availability and quality of sampled data, and the geological complexity of the deposit. Since geostatistical modeling relies on sampling data, it is crucial to follow established industry standards in logging, sampling, and data management. Failing to do so introduces bias and reduces reliability (Rossi & Deutsch, 2014; The Australasian Institute of Mining and Metallurgy, 2014).

## 2.2 Geostatistical Methods and Their Applications

A wide range of mineral commodities can be modeled using geostatistical methods, including industrial minerals, base and precious metals, coal, and diamonds (Rossi & Deutsch, 2014); moreover, it is possible to model and estimate grade, ore reserves (Afeni, Akeju, & Aladejare, 2021), concentration (Njayou, Foba-Tendo, Boukong, & Sigha-Nkamdjou, 2023), geological (Fouepe Takounjou et al., 2022), geotechnical (Khan, Khan, Khan, & Qureshi, 2016), hydrogeological (Srisuk, Chotpantarat, & Ongsomwang, 2023), and metallurgical parameters (Abildin, Madani, & Topal, 2018; Zhexenbayeva et al., 2024). The geostatistical modeling methods are generally classified as either deterministic or stochastic. Deterministic approaches rely on fixed spatial relationships between data points and do not account for uncertainty, especially in areas with sparse sampling. Common deterministic interpolation methods include Inverse Distance Weighting (IDW), Nearest Neighbor, and Kriging, which assign values based purely on proximity or fixed rules without modeling spatial variability. In contrast, stochastic methods incorporate spatial dependence through random functions, allowing for the generation of multiple equally probable realizations. These realizations help quantify uncertainty and are particularly useful in geostatistical modeling. Kriging provides a best linear unbiased estimator of unknown values based on known sample points and their spatial correlation structures. However, it suffers from smoothing effects that can misrepresent high or low values within the modeled domain (Goovaerts, 2016). Common stochastic simulation techniques include Sequential Gaussian Simulation (SGS), Turning Bands Simulation (TBS), and Multiple-Point Simulation (MPS). These approaches preserve the statistical properties of the original data and better capture spatial heterogeneity. Selecting the appropriate method depends on the nature of the variable, the spatial structure of the data, and the objectives of the study. When modeling non-additive or highly variable parameters, stochastic approaches are often preferred due to their ability to represent uncertainty and local variability.

## 2.3 The Role and Importance of Variogram Analysis in Geostatistical Modeling

Variograms are essential tools in geostatistics as they describe the spatial continuity and dependence of a variable by quantifying how the similarity between data points decreases with distance. The experimental variogram, calculated from sample data, is used to model the spatial structure and informs key interpolation techniques such as kriging (Goovaerts, 2016; Wackernagel, 2003). This model is fundamental for predicting values at unsampled locations and plays a pivotal role in reducing estimation errors and improving model reliability. A well-fitted variogram captures the nugget effect, range, and sill, which define the scale of spatial correlation and variability within a dataset (Goovaerts, 2016). For accurate geostatistical modeling, especially in mining and environmental studies, selecting and fitting a suitable variogram model is crucial, as it directly influences the quality of interpolated surfaces and associated uncertainty (Bai & Tahmasebi, 2022). Ignoring spatial correlation or using a poorly constructed variogram can result in biased estimates and the misrepresentation of geological features. Thus, variogram analysis is a cornerstone of spatial data interpretation and resource estimation across geoscientific disciplines.

## 2.4 The Challenge of Non-Additive Variables

Non-additive variables pose significant challenges in geostatistical modeling due to their inability to be averaged or linearized across geological domains. Unlike additive variables such as volume or mass, non-additive variables - including grade, metallurgical recovery, and certain geotechnical or mineralogical properties - cannot be summed or averaged over larger blocks without introducing bias. This issue becomes particularly problematic when using traditional kriging techniques, which assume additivity and stationarity, leading to the smoothing of high and low values and resulting in the underestimation of extremes - a phenomenon known as the “smoothing effect” (Carrasco et al., 2008; Adeli et al., 2021). The challenge of non-additivity also affects the concept of support, referring to the scale or volume over which a variable is measured or estimated. Variables such as grade multiplied by density (e.g., $Fe \times \rho$) may behave additively, whereas individual grades may not, necessitating transformations or alternative modeling approaches like co-kriging or co-simulation-based methods. To address the issue of the non-additive variables in the geostatistical modeling, various techniques are employed. For example, sequential Gaussian simulation (SGS) and sequential Gaussian co-simulation (SGCS) are often implemented to model the non-additive variables due to the better ability to capture spatial variability and uncertainty while preserving the original data's histogram and variogram structures (Boisvert et al., 2009; Goovaerts, 2016). Recent research has proposed methodologies to handle non-additive variables more effectively. For instance, a study introduced a Gibbs Sampler approach for modeling metallurgical recovery, addressing change of support problems through additive auxiliary variables (Carrasco et al., 2018). Another approach involves the direct simulation of non-additive properties on unstructured grids, allowing more accurate modeling of complex geological features (Mourlanette et al., 2020). Furthermore, modeling non-additive variables in domains like tailings storage facilities or ore bodies becomes more complex due to preferential sampling, heterogeneity, and lack of statistical stationarity, which violate assumptions in classical geostatistics. Addressing these challenges requires careful consideration of data transformations, estimation support, and simulation techniques to produce realistic and unbiased spatial models (Adeli et al., 2021). In summary, the geostatistical modeling of non-additive variables demands specialized techniques and a thorough understanding of the underlying geological processes to ensure accurate resource estimation and decision-making in mining and related fields.

## 2.5 Importance of Support Systems

Geostatistical modeling frequently involves the concept of "support," referring to the size, shape, and orientation of the area or volume from which spatial measurements are obtained. According to Goovaerts (2016), the term "support" defines the spatial scale—such as length, area, or volume—associated with each measurement, significantly influencing the outcomes of geostatistical analyses. Point support refers to data collected at individual, precise locations with negligible spatial extent. These often include drill hole assays, soil samples, or other spot measurements commonly utilized in geological exploration and environmental monitoring. While point support data are straightforward, computationally simple, and quick to analyze, they inherently fail to capture variability within larger blocks or spatial domains. This limitation becomes especially pronounced when dealing with spatially heterogeneous variables, leading to potential underestimation of variability within the modeled domain and, consequently, misrepresentation of the spatial distribution (Carrasco, Chiles, & Seguret, 2008). This smoothing effect, prevalent in point-supported models, reduces the accuracy of predictions in resource estimation and geological characterization. In contrast, block support involves aggregating data over defined volumes or areas, representing an average or composite value for the variable of interest. Typically, this involves discretizing larger spatial domains into smaller sub-blocks, each contributing to a collective estimate for the entire block (Emery & Ortiz, 2011). Block support addresses many of the shortcomings associated with point support, particularly by providing a more representative and realistic measure of variability across heterogeneous areas. Although computationally more demanding, block support yields higher accuracy and reduces smoothing effects through improved local variability representation. Furthermore, block-support variograms exhibit reduced variance compared to point-support variograms due to averaging effects, emphasizing the importance of correct variogram modeling for precise spatial estimation (Goovaerts, 2016). The transition between point and block support introduces the "change of support problem," as statistical distributions of spatial variables alter significantly when aggregating or disaggregating data between different scales (Boucher & Dimitrakopoulos, 2012). Despite higher computational intensity, the application of block support techniques significantly enhances geostatistical modeling results and their reliability, especially in mining and environmental sciences, by effectively capturing spatial variability (Carrasco, Chiles, & Seguret, 2008; Emery & Ortiz, 2011).

## 2.6 Tailings Modeling

Modeling Tailings Storage Facilities (TSFs) poses significant challenges for geostatistical approaches, primarily due to intrinsic heterogeneity, data limitations, and post-depositional alterations. One critical issue is the variable deposition practices throughout the lifetime of a TSF. Changes in tailings disposal techniques, driven by technological advancements or operational adjustments, cause pronounced spatial variability within the deposited materials, complicating consistent representation in geostatistical models (Blannin et al., 2023; Lottermoser, 2010). This variability often violates traditional assumptions of spatial stationarity, posing serious challenges for standard kriging approaches, which assume consistent statistical properties across space (Carrasco, Chiles, & Seguret, 2008). A second major issue arises from the heterogeneous particle settling processes within TSFs. Tailings slurry deposition naturally causes particle sorting by size and density, creating distinct sediment layers with contrasting geochemical and mineralogical characteristics (Khalil, Koucham, & El-Adnani, 2023). This stratification leads to pronounced vertical and horizontal anisotropy, often requiring advanced modeling methods such as anisotropic variograms or directional simulations to accurately reflect spatial correlations (Blannin et al., 2023). Failure to incorporate this anisotropy into geostatistical models can result in biased estimates, underestimating or overestimating the actual mineral content. Another considerable challenge is the chemical and mineralogical alterations that tailings undergo due to weathering processes. Oxidation, hydrolysis, and leaching significantly modify the original tailings composition, which can shift the statistical properties of the sampled materials over time, reducing the reliability of models based solely on historical data (Kossoff et al., 2014; Khalil et al., 2023). To account for this, recent geostatistical studies recommend integrating geochemical modeling and sequential Gaussian co-simulation methods, enabling the generation of multiple realizations that reflect possible geochemical transformations and better represent uncertainty (Blannin et al., 2023). Additionally, the accuracy of geostatistical models of TSFs is severely limited by data scarcity and outdated sampling. Historical sampling campaigns often lack detailed information regarding ore properties, processing methods, or spatial sampling density, increasing uncertainty in models developed from these datasets (Edraki et al., 2014). Addressing this requires comprehensive, modern sampling protocols and possibly supplementing historical data with contemporary geophysical surveys or remote sensing techniques, which enhance data availability and spatial resolution, consequently improving model precision (Khalil et al., 2023; Kossoff et al., 2014). To effectively overcome these challenges, recent literature emphasizes using advanced geostatistical simulation methods—particularly Sequential Gaussian Simulation (SGS), Universal Kriging-based simulations, and co-simulation techniques—which can explicitly account for spatial variability, anisotropy, and uncertainty, providing more robust and reliable TSF models (Blannin et al., 2023; Khalil et al., 2023).

## 2.7 Kriging Approaches for Non-Additive Variables

Kriging is widely used as a deterministic interpolation method. However, traditional kriging approaches—simple and ordinary kriging—often struggle to manage non-additive variables effectively. According to Adeli et al. (2021), simple kriging performed inadequately in their study, largely due to its inability to accurately recreate the relationship between primary and secondary variables, as it excludes the covariate information from calculations. This resulted in significant discrepancies, such as mismatches in the mean value of the primary variable, primarily attributed to uneven sample distribution. To address this, declustering techniques are recommended to enhance representativity and accuracy.

Ordinary cokriging also demonstrated limitations, generating incomplete models and estimating values only near existing data points. This was mainly due to insufficient data coverage for the primary variables. Additionally, this method occasionally yielded extremely high estimated values that were not representative of the true spatial distribution, rendering the results unreliable for practical applications (Adeli et al., 2021). To overcome these limitations, cokriging methods incorporating known linear combinations of means were introduced, showing significant improvement in handling areas with sparse primary data, providing estimates closer to initial data means, and yielding unbiased outcomes.

As an additional alternative to the traditional techniques for overcoming the non-additive behavior of variables, Indicator kriging has been suggested. Especially when those variables show significant non-linearity or fall into multiple categories, such as varying quality levels. Indicator kriging forecasts the probability that a variable will surpass specified thresholds, as opposed to estimates of continuous values. By transforming the raw data into binary indicators, the effective spatial distribution of threshold-based or categorical features is demonstrated. RQD values in rock mass quality mapping can be classified as extremely poor, poor, fair, good, and exceptional, while indicator kriging can assess each category's probability independently. The impact of smoothing effect can be decreased, and local variability can be more accurately reproduced than with ordinary kriging, even though indicator kriging requires careful threshold selection and typically involves modeling multiple indicator variograms, increasing workflow complexity (Madani et al., 2018; Goovaerts, 1997).

## 2.8 Sequential Gaussian Simulation (SGS)

Stochastic simulation methods such as Sequential Gaussian Simulation (SGS) offer alternative solutions by incorporating uncertainty and variability through multiple equally probable realizations. SGS has generally exhibited robust performance in reproducing original histograms and variogram structures. For instance, the study by Shademan and Farhadian (2023) successfully applied SGS to model the Geological Strength Index (GSI), achieving accurate reproduction of spatial distribution patterns, especially in areas with significant geological discontinuities.

## 2.9 Sequential Gaussian Co-simulation (SGCS)

SG Co-simulation theoretically offers advantages by integrating secondary data into the modeling process. However, it demonstrated poor performance in the study conducted by Boisvert, Rossi, and Deutsch (2009). The limitations were heavily impacted by the presence of secondary variables and high dependence on them, coupled with sparse sampling of primary variables, which compromised the accuracy of histogram and variogram reproduction.

## 2.10 Comparative Summary

In summary, the choice of geostatistical methodology significantly impacts the modeling of non-additive variables. Traditional kriging-based methods provide a foundational interpolation approach but frequently struggle with the complexities introduced by non-additivity and sparse data distributions. Advanced kriging methods, like cokriging with known linear combinations, significantly mitigate some of these issues. Nevertheless, stochastic simulations, notably SGS, often provide superior outcomes in representing the true variability and uncertainty of spatial data, particularly when complemented by adequate sampling strategies and supplementary analytical techniques.

Table 1. Summary of geostatistical methodologies for modeling non-additive variables.

| Methods | Performance summary | References |
|---|---|---|
| Kriging methodologies | | |
| Simple Kriging (SK) | Poor reproduction: failed to accurately represent the relationship between primary and secondary variables due to the exclusion of covariates. | Adeli et al. (2021) |
| Ordinary Kriging (OK) | Applied as a linear estimation method assuming local stationarity. Failed to account for the non-additive nature of geometallurgical variables. Produced smoother models with underestimated high values and overestimated low values, leading to biased reconciliation results. | Garrido et al. (2019); Leal et al. (2016) |
| Ordinary | Generated incomplete models; estimated points | Adeli et al. |

| | | |
|---|---|---|
| Cokriging | predominantly near existing data points, resulting in unrealistically high values in sparse regions. | (2021) |
| Cokriging with means related by linear combinations | Successfully addressed limitations of other cokriging methods, effectively handling sparse data. Produced unbiased results with estimates closely matching input data. | Adeli et al. (2021) |
| Multi-Gaussian Kriging | Applied to map non-additive variables like RQD. Improved local variability representation and reduced smoothing effects. Enabled uncertainty quantification through conditional distributions. Model validation confirmed effective spatial reproduc | Madani et al. (2018) |
| Indicator Kriging | Successfully addressed limitations of linear methods by transforming variables into indicators. Enabled probability-based estimation at cut-off thresholds. Provided more accurate block model predictions and showed better alignment with processing plant results. | Leal et al. (2016) |
| Simulations | | |
| Sequential Gaussian Simulation (SGS) | Provided generally robust results and reproduced initial histograms and variogram structures accurately, which is especially beneficial for modeling variables with significant spatial discontinuities. | Shademan & Farhadian (2023) |
| Sequential Gaussian Co-simulation (SGCS) | Showed poor performance; weak representation of initial data distributions due to heavy reliance on sparsely sampled primary variables. | Boisvert, Rossi, & Deutsch (2009) |

# 3. METHODOLOGY

The primary aim of this study is the conducting of geostatistical modeling with its further analysis, and integration of the block support principle, its application in modeling mine tailings, and the implementation of sequential Gaussian co-simulation (SGCS) for non-additive variables, focusing on iron (Fe) grade distribution across various grid resolutions of the mine tailings. Iron grade is classified as a non-additive variable, which presents an additional challenge for geostatistical modeling (Carrasco, Chiles, & Seguret, 2008; Adeli et al., 2021). The analysis emphasizes the importance of accounting for support effects when transitioning from point-support to block-support estimates, particularly in heterogeneous environments like tailings storage facilities and when modeling non-additive variables (Goovaerts, 2016; Madani & Emery, 2015). By integrating SGCS, the study captures the spatial variability and cross-correlations of multiple variables, enhancing the reliability of resource assessments (Boisvert, Rossi, & Deutsch, 2009; Liu, Xia, & Cheng, 2023). For this study, different grid sizes were used, which allowed an evaluation of scale-dependent behavior, offering insights into the optimal resolution for both modeling and potential resource recovery strategies (Blannin et al., 2023).

Qualitative modeling of iron grade within tailings storage facilities (TSFs) presents numerous challenges, and only a limited number of studies have specifically addressed this topic. A primary issue is the high degree of heterogeneity within the tailings. Tailings are typically deposited as slurry, undergoing sedimentary-type deposition that causes particles to settle based on size and density. This process results in a spatially heterogeneous, stratified structure with variable-grade regions (Blannin et al., 2023; Koucham et al., 2024). Additionally, factors such as ore processing methods, deposition techniques, and the location of spill points critically influence the spatial distribution of grade values. Furthermore, iron grade is a non-additive variable, meaning it cannot be averaged linearly across space, especially at block scales or within the distribution extremes, such as the first and fourth quartiles (Shademan & Farhadian, 2023; Carrasco, Chiles, & Seguret, 2008; Goovaerts, 2016). This non-additivity introduces nonlinear relationships between sample values and their block-scale equivalents. If these nonlinearities are ignored, geostatistical models risk underrepresenting variability and may lead to incorrect classification of material as ore or waste (Boisvert, Rossi, & Deutsch, 2009). The complexity is further aggravated by lithological heterogeneity and internal microstructures, such as grain size, porosity, and mineral locking, which influence the geometallurgical behavior of the iron grade (Chen, 2022). Consequently, effective modeling in such environments requires a robust multivariate geostatistical strategy. Integrating block support with co-simulation methods allows for better representation of spatial variability and cross-correlations, ultimately improving the reliability of both resource recovery forecasts and environmental assessments (Emery & Ortiz, 2011; Goovaerts, 1997).

## 3.1 Sequential Gaussian Co-Simulation

SGCS is a powerful geostatistical technique that enhances the traditional sequential Gaussian simulation (SGS) by incorporating one or additional auxiliary spatial variables. The SGS was developed in the late 1970s and early 1980s by the A. Journel and C. Huijbregts at Stanford University, it was designed to model spatial uncertainty by implementing the methodology of generating equally probable realizations for a single Gaussian-distributed variable (Gómez-Hernández & Srivastava, 2021). SGCS gained traction through the contributions of Goovaerts (1997), who provided a systematic framework for its application to multivariate spatial datasets. The method assumes that the primary and secondary variables can be transformed into standard Gaussian distributions and that their joint spatial behavior can be described through a combination of direct and cross-variograms that conform to the Linear Model of Coregionalization (LMC).

The key assumptions of SGCS are:

- All involved variables are normally distributed after transformation.
- Spatial stationarity holds within local neighborhoods.
- Direct and cross-variograms must conform to a shared spatial structure via the LMC.

Non-additivity stands as a critical challenge for geostatistical modeling. Due to the inability to be linearly averaged, they significantly complicate the modeling accuracy. It could be solved by various techniques that solve the non-additivity. The SGCS is one of the techniques that can overcome the issues related to the modeling of the non-additive variables. This challenge is mitigated through the integration of a secondary variable, which serves as auxiliary information to improve the quality and reliability of the estimation. The inclusion of such auxiliary variables enhances precision, preserves spatial variability, and enables uncertainty quantification (Goovaerts, 1997; Gómez-Hernández & Srivastava, 2021). The SGCS methodology involves the construction of a random path through all grid nodes. At each node, the method identifies nearby sampled data. A conditional distribution is then estimated using cokriging, from which the value for the center of the block is obtained. This process is repeated until all blocks are simulated. Once the simulation is complete, the results are back-transformed to their original data scale to evaluate the resulting model. An alternative approach is the hierarchical simulation of variables, proposed by Almeida and Journel (1994). This method involves simulating variables in a pre-defined order based on a hierarchical structure and allows the use of full cokriging, collocated cokriging approximations, or approximations based on the Markov-Bayes model. Another approach, proposed by Luster (1985), focuses on transforming correlated variables into uncorrelated ones by decomposing the original dataset into orthogonal factors using principal component analysis (PCA). This method assumes that the orthogonality observed at lag zero is maintained across all spatial lags. Further alternatives include the use of a super-secondary variable (Babak & Deutsch, 2009) or stepwise conditional transformation (Leuangthong & Deutsch, 2003). The choice between these depends on the nature of the relationship between the primary and secondary variables. When the relationship is primarily linear, the super-secondary variable approach is preferred. However, in the cases of non-linear or constrained relationships, the stepwise conditional transformation offers a more flexible and effective solution (Rossi & Deutsch, 2014).

The cross-variogram is an essential part of conducting the SGCS, and it is used to represent the spatial coregionalization model between the variables. In other words, a cross-variogram is a tool that can describe the spatial variability between the two variables over the distance between the samples. The following formula is used to estimate and construct a cross-variogram:

$$\gamma_{jj} = \frac{\Sigma_{a=1}^{n(h)}[z_i(x_a) - z_i(x_a + h)] \times [z_j(x_\alpha) - z_j(x_\alpha + h)]}{2n(h)} \tag{1}$$

Where $\gamma_{ij}(h)$ is the cross-variogram value at lag h, between two regionalized variables $z_i$ and $z_j$, $n(h)$ is the number of paired data points separated by the lag vector h, $z_i(x_\alpha)$ and $z_j(x_\alpha)$ are the observed values of variables i and j, respectively to the location of $x_\alpha$, $z_i(x_\alpha + h)$ and $z_j(x_\alpha + h)$ are the observed values of variables i and j at the location separated by vector h from $x_\alpha$

Moreover, the SGCS approach, to estimate any single node to be simulated, implements the direct simple cokriging estimation methodology, which means that newly simulated values are not added to the conditioning dataset and are not used for further estimations. The simple cokriging estimator is obtained by the following formula:

$$z^*(u) - m_z = \sum_{\alpha_1=1}^{n_1(u)} \lambda_{\alpha_1}(u)[z(u_{\alpha_1}) - m_z] + \sum_{\alpha_2=1}^{n_2(u)} \lambda'_{\alpha_2}(u)[z(u'_{\alpha_2}) - m_y] \tag{2}$$

Where $z^*(u)$ is the estimated (simulated) value of the primary variable at location u, $m_z$ and $m_y$ are the means of the primary and secondary variable, both of them are assumed to be known, $\lambda_{\alpha_1}$ and $\lambda'_{\alpha_2}$ are the weights assigned to the $\alpha$-th primary and secondary variables respectively, $z(u_{\alpha_1})$ and $z(u'_{\alpha_2})$ are the values of the primary and secondary variables at locations $u_{\alpha_1}$ and $u'_{\alpha_2}$ respectively, $n_1(u)$ and $n_2(u)$ are the numbers of primary and secondary variables respectively at the estimation u.

## 3.2 Block Support Implementation for the SGCS

By integrating block support into SGCS, the reliability of the obtained model is significantly enhanced, especially for the modeling of the non-additive variables such as metal grade or metal recovery (Carrasco et al., 2008; Emery & Ortiz, 2011; Goovaerts, 1997). Unlike the point support, which estimates the variable value at the center of the block, the block support discretized the block into sub-blocks and, with further averaging, the simulated values of the center of sub-blocks. Implementation of this approach allows to effectively capture the internal heterogeneity and reduce the variance of the simulated realizations. Despite the improved estimation and better uncertainty quantification of the block support, it has several drawbacks. Due to the larger number of estimations required for each block, computational time and requirements are increased. Additionally, the averaging of the sub-blocks leads to the reduction of the local extremes, which potentially may underestimate the higher values and overestimate the lower values (Goovaerts, 1997; Leuangthong & Deutsch, 2003).

## 3.3 Additive Variable Estimation for the SGCS

To implement SGCS for modeling non-additive variables, the chosen methodology suggests the derivation of a variable with the additive behavior, the so-called additive proxy. Instead of a non-additive variable, a proxy would have an additive behavior, which allows obtaining an unbiased and reliable geostatistical model. The additive proxy must be derived from a primary variable that was initially aimed to be modeled so it could be back-transformed to the original scale. In case of the modeling of such variables like grade, which behave non-additively, the sufficient proxy would be a multiplication of a grade on the density.

$$Additive\ proxy = Metal\ grade \times Density \tag{3}$$

The product of metal grade and density approximates the mass or content of metal per unit volume, which will be an additive quantity. After the simulation, the metal grade could be estimated by back-transorming through reversing the formula 3.

Such an approach requires the density variable. However, density is not usually estimated during the sampling operation, especially in the exploratory stages. Thus, density must also be calculated by using theoretical and empirical formulas. In 2023, Blannin et al. suggested a methodology for density estimations, where they aimed to assess the Davidschacht TSF.  This methodology is based on the geochemical and mineralogical composition and the porosity. Afterward, the bulk density was obtained for the further modeling of TSF. Another way to calculate density is based solely on the geochemical composition and is more simplified when compared to the Blannin methodology.

$$\text{Density} = \Sigma\ (\text{Element Fraction} \times \text{Element Density}) \tag{4}$$

Where the Element Fraction is derived from its grade or content. Even though this density calculation technique is less accurate than the Blannin et al. methodology proposed in 2023, this method provides an approximate density and is especially useful in case the mineralogical data is absent.

# 4. RESULTS

## 4.1 Case Study

The SGCS methodology with the integration of a block support system was applied to the Haveri copper gold porphyry mine tailings deposited over 60 years ago in SW Finland (Parviainen, Soto, & Caraballo Monge, 2020). The dataset included the values from two sampling operations. The first sampling operation was conducted in 1980, consist of 192 samples, and included the values for the following chemical elements: Silver (Ag) in ppm, Arsenic (As) in ppm, Gold (Au) in ppm, Cobalt (Co) in ppm, Copper (Cu) in ppm, Iron (Fe) in %, Nickel (Ni) in ppm, Lead (Pb) in ppm, Sulphur (S) in %, and Zinc (Zn) in ppm. The second sampling operation was conducted in 1983, containing 922 values for Ag, As, Au, Co, Cu, and Fe. Overall, the dataset included 1114 sample measurements for various chemical elements within the Haveri tailings facility.

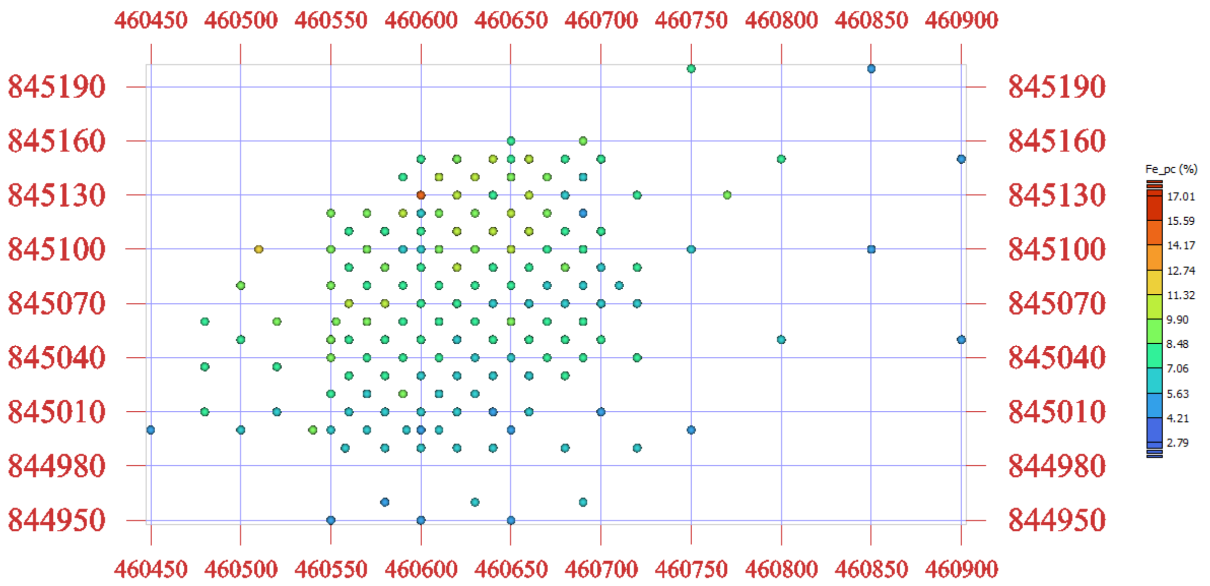


Figure 1. 2D location map of drillholes showing Fe (%) grades across TSF.

Figure 1 represents the 2d spatial distribution of Fe grade values obtained from drillhole sampling across Haveri TSF. The color gradient illustrates the variability in iron grade, where the dark-red to yellow colors represent higher concentrations, and green to blue colors indicate lower values of the Iron grade. According to the map, the central-western region contains higher Fe grades, approximately 13-15%, whereas the lower Iron grade concentrations are in the eastern and southern boundaries of the dataset. Such spatial heterogeneity reflects the impact of the deposition patterns used during the operational period of the mine. The higher Fe grade zones are clustered within specific areas, which is suggested to be a result of a preferential deposition and settling by density of the waste material.

## 4.2 EDA Analysis

The Iron grade, which is the variable of interest, has overall 1114 sample values. The statistical parameters of the Iron grade could be extracted from table 2.

Table 2. Sampled Fe grade statistical parameters.

| | Mean | Variance | Std. Dev | Minimum value | Maximum value |
|---|---|---|---|---|---|
| Sampled Fe grade | 10.02% | 4.664%$^2$ | 2.16% | 2.79% | 17.01% |

Overall, the sampled data contain approximately high average value of the Iron grade, w with the moderate variability across the dataset, with the presence of enriched and low-grade zones

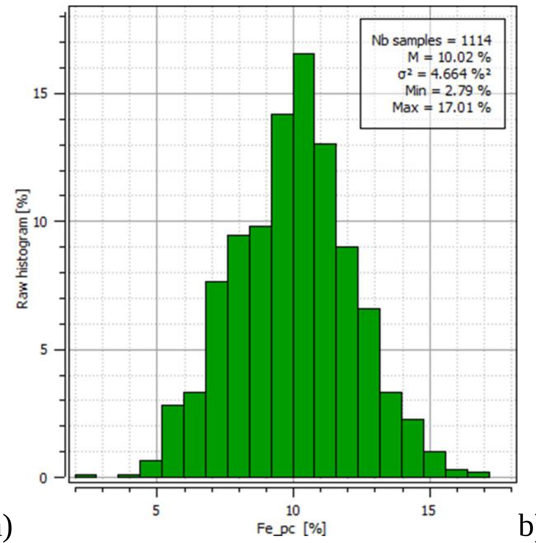


a)

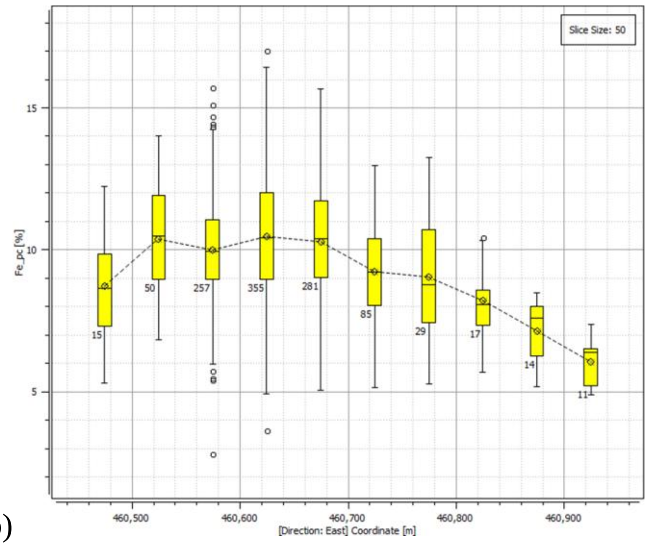


b)

c) 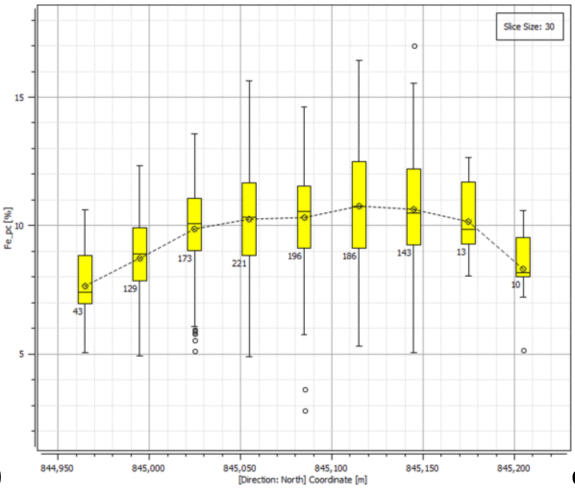


d) 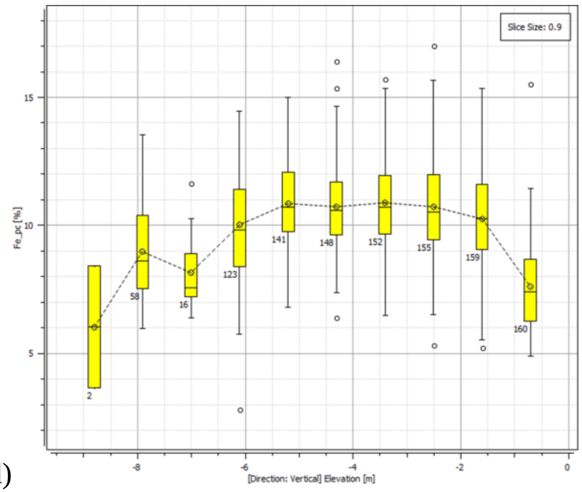


Figure 2. Iron grade properties: a) histogram, b) swath plot with east direction, c) swath plot with north direction, and d) swath plot with vertical direction

In Figure 2a, the histogram of the Fe grade shows a positively skewed distribution, with a notable peak around 9-11%, which indicates that most of the data contain moderate grade values, and the high-grade values are comparably rare.  In Figures 2b, 2c, and 2d, the swath plots across 3 directions are present, east, north, and vertical, respectively, with the figure names.  Figure 2b, with an east direction, shows a noticeable variability, with a higher grade concentration within the 460,500 to 460,700 m coordinates along the east direction.  In Figure 2c, the average grade stays approximately on the same level from 845,020 to 845,180 m coordinates, decreasing the values at the northern and southern boundaries. In the vertical direction, Figure 2d, the Fe grade gradually increases with depth, suggesting a density sorting of heavier iron-bearing particles during deposition.

## 4.3 Additive variable estimation

As the proposed methodology in the Methodology section 3.3, it is required to estimate an additive proxy. In this case, our goal is to model an Iron grade, which is a non-additive variable. Instead of directly modeling the Irong grade, the additive proxy of Fe*density could be implemented, but initially, it is important to estimate the density component.

The Haveri dataset does not contain both density and mineralogical data. Therefore, the simplified methodology based on the weighted average approach was chosen for the density calculations, which is shown in formula 4.  Initially, it was necessary to obtain the fraction of each element. To achieve this:

- Elements reported in PPM were divided by 1,000,000.

- Iron and Sulfur, which were reported as percentages, were divided by 100.

$$\text{Elements fraction} = \text{Element in PPM} / 1000000 \tag{5}$$

$$\text{Element fraction} = \text{Element in \%} / 100 \tag{6}$$

Calculation example:

If Cu_PPM is 452 PPM

$$\text{Cu fraction} = 452 / 1000000 = 0.000452$$

If Fe_pc is 5.29%

$$\text{Fe fraction} = 5.29 / 100 = 0.0529$$

These fractions represent the proportion of each element at a given point in a drill hole. These values are then multiplied by their respective standard densities (in g/cm$^3$) and summed based on the following formula.

$$\text{Density} = \Sigma\ (\text{Element Fraction} \times \text{Element Density}) \tag{4}$$

The elements' densities used in the calculation are presented in Table 3. These values were obtained from an open-source reference and represent standard room-temperature densities in g/cm$^3$.

Table 3. Standard densities of chemical elements.

| Element | Density (g/cm$^3$) |
|---|---|
| Silver (Ag) | 10.49 |
| Arsenic (As) | 5.73 |
| Gold (Au) | 19.32 |
| Cobalt (Co) | 8.90 |
| Copper (Cu) | 8.96 |
| Iron (Fe) | 7.87 |
| Nickel (Ni) | 8.91 |
| Lead (Pb) | 11.34 |

| | |
|---|---|
| Sulfur (S) | 2.07 |
| Zinc (Zn) | 7.14 |

Heavier elements, like gold (19.32 g/cm³), lead (11.34 g/cm³), and silver (g/cm³), contribute more significantly to the calculated density, while lighter elements like sulfur (2.07 g/cm³) have a comparatively smaller impact on the density estimations. Such an approach allows us to obtain more realistic results for the density. Even though nickel, lead, sulfur, and zinc values were available for only 193 sample points from the first sampling operation, they were also included for the estimation of density. However, the chemical composition is incomplete; thus, the missing elements were neglected to estimate density in the remaining sample points. After completing all computations, the minimum and maximum density values яwere 0.238 g/cm³ and 1.372 g/cm³, respectively, with an average density of 0.826 g/cm³. To adjust the density to a more realistic range typical of soil-type materials, a rescaling formula was applied.

$$\text{Normalized Density} = 1 + [(\text{Density} - \text{Min Density}) / (\text{Max Density} - \text{Min Density})] \times (2 - 1) \tag{7}$$

The new density range was set between 1 and 2 g/cm³ to ensure a representative average density while minimizing the impact of extreme scaling and preserving the physical plausibility of the data. Afterward, the density was converted into kg/m$^3$. The mean value of the normalized density is 1517.48 kg/m$^3$, variance is 22596 1517.48 (kg/m$^3$)$^2$, Std. Dev is 150.32 kg/m$^3$, Minimum value 1000 kg/m$^3$, and Maximum value of 2000 kg/m$^3$, which could be observed in Figure 3.

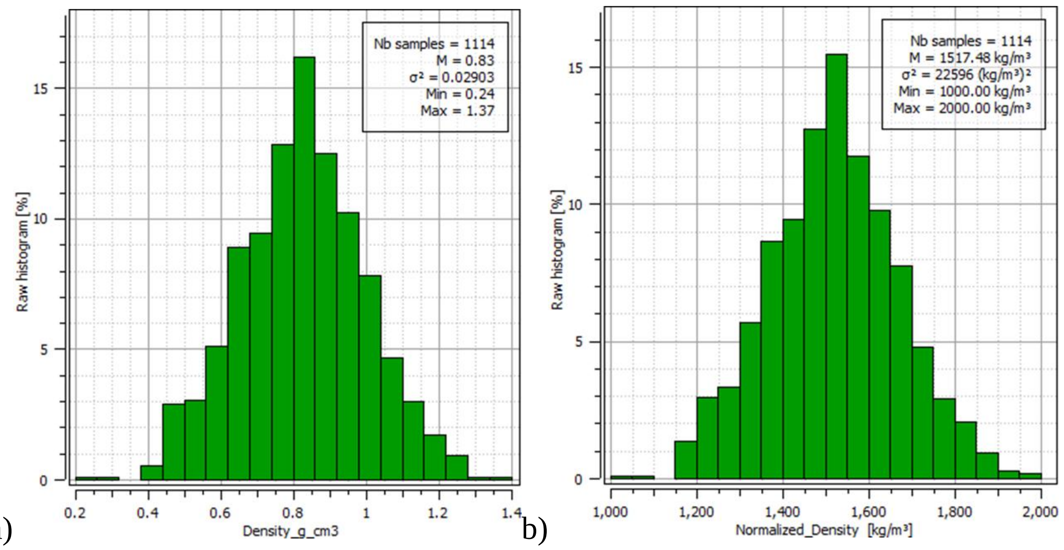


Figure 3. Density variables, a) density before normalization, b) density after normalization

Figure 3 illustrates the calculated density distribution before normalization (Figure 3a) and after normalization (Figure 3b). The resulting models for both histograms are approximately symmetric and unimodal, whereas most of the density before normaliztion was around a mean of 0.83 g/cm$^3$ and 1520 kg/m$^3$ respectively.

After obtaining the Normalized density, it was able to obtain the additive proxy, Fe*density, by using the formula 8.

$$Fe * density = Fe \times Normalized\ density \tag{8}$$

## 4.4 SGCS justification

To overcome the issue of non-additivity in the Fe grade, an additive proxyб the product of Fe and density (Fe*density), was introduced. This transformation allows the modeling of an additive variable that is more appropriate for block-support simulation (Carrasco, Chiles, & Seguret, 2008; Goovaerts, 1997). However, to recover the original Fe grade values after simulation, the density must also be simulated along with Fe*density. Where the density would be a secondary variable. This requirement leads to the use of co-simulation, which allows both variables to be modeled simultaneously while preserving their spatial correlation. Among available techniques, sequential Gaussian co-simulation is one of the most robust and widely used methodologies for modeling correlated, multivariate spatial data (Goovaerts, 1997; Rossi & Deutsch, 2014). SGCS not only maintains the statistics of the variables and spatial variability of each individual variable but also ensures that their joint spatial structure, which is quantified through cross-variograms, is retained throughout the simulation (Boisvert, Rossi, & Deutsch, 2009). This makes SGCS particularly suitable for resource estimation, especially in this case.

## 4.5 Cross-Variogram Modeling

Before applying SGCS, it is essential to evaluate and model the spatial relationship between the primary variable (Fe*density) and the secondary variable (Normalized density). This is achieved through the construction of a cross-variogram, which quantifies the degree of spatial correlation between the two variables as a function of separation distance. To ensure compatibility with the Gaussian assumptions of SGCS, both variables were first transformed into the Gaussian domain using normal score transformation. Following this, experimental direct variograms for Fe* density and normalized density were computed to assess their spatial structure (Figures 4a and 4b). Experimental direct variograms are estimated by the following formula:

$$\gamma(h) = \frac{1}{2n(h)} \sum_{i=1}^{n(h)} [z(x_i) - z(x_i + h)]^2 \tag{9}$$

A cross-variogram was calculated ssimultaneouslybetween the two transformed variables (Figure 4c). The cross-variogram formula is calculated by formula 1:

$$\gamma_{jj} = \frac{\Sigma_{a=1}^{n(h)} [z_i(x_a) - z_i(x_a + h)] \times [z_j(x_\alpha) - z_j(x_\alpha + h)]}{2n(h)} \tag{1}$$

During this process, the variogram values were normalized such that the sill equals 1, ensuring proper comparison and fitting under the LMC framework. The variograms and cross-variogram were modeled in two principal directions: horizontal (0°) and vertical (90°). This directional analysis is a necessary part to determine the anisotropic nature within the tailings deposit. Which ooccurreddue to the preferential deposition anddensity-basedd settling within the tailings facility. The vertical direction is required since,the particles were settled by the densities, resulting in layering and vertical stratification. The horizontal direction reflects the variations in deposition zones and flow ppatternsover time. The two principal directions would capture the geological anisotropy within the tailings facility, allowing for a more accurate representation of spatial continuity for the co-simulation

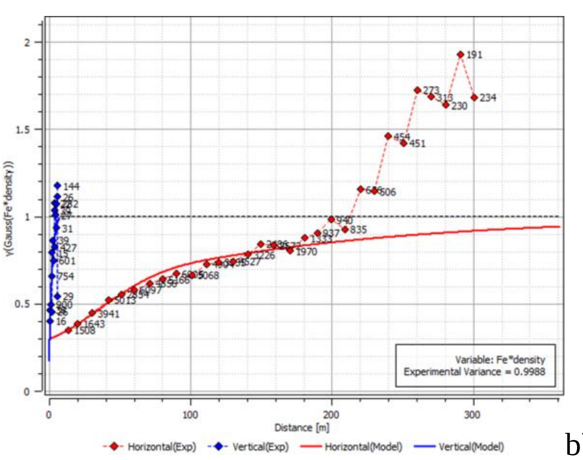


a)

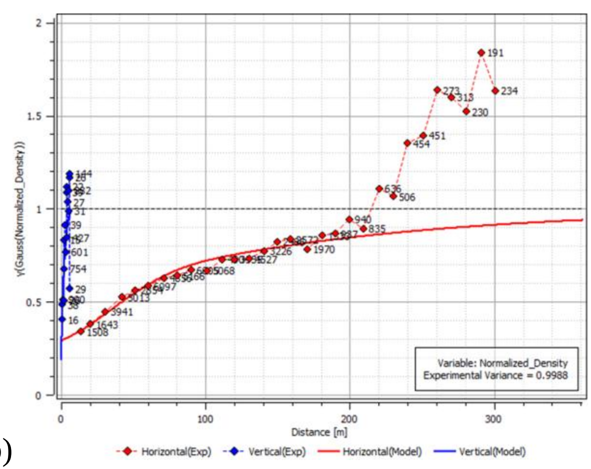


b)

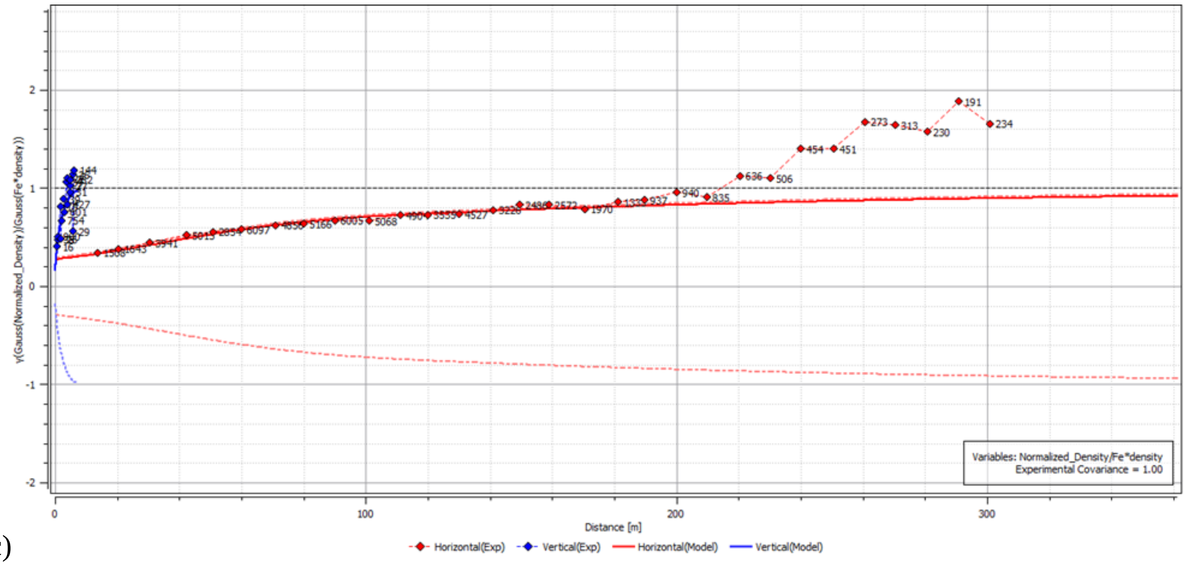


c)

Figure 4. Direct variograms for a) Gaussian Fe*density, b) Gaussian Normalized density, c) Cross-variogram between Gaussian Fe*density and Gaussian Normalized density

## 4.6 Sequential Gaussian Co-Simulation

To model the spatial variability of the Fe grade with improved accuracy and uncertainty quantification, Sequential Gaussian Co-Simulation (SGCS) with block support was applied. The SGCS was performed using two different block grid resolutions: 5×5×1 m and 10×10×1 m. For each grid, 100 realizations were generated for both the Fe*density (primary variable) and Normalized density (secondary variable). These simulations were conducted slice-wise, with a focus on slice 7, which represents a horizontal section of the tailings storage facility (TSF) at a fixed vertical depth.

Each co-simulation output includes:

- Mean maps (E-type maps) - showing the average value across all realizations
- Variance maps - representing the spatial uncertainty
- Individual realizations – illustrates potential spatial distributions of the variables from a simulation

Figures 5a-5e display the result of the Fe*density co-simulation output over a 5x5x1m grid. Figure 5a displays the mean map of the Fe*density,  derived by averaging all 100 realizations. This map shows consistent zones with high values of the Fe*density, particularly in the central part of a TSF. The smoother transitions and well-defined zones reflect the effect of block averaging and the robustness of the co-simulation. Figure 5b shows the variance map, identifying areas with high simulation uncertainty. In this figure, the boundaries and the under-sampled zones correspond to higher uncertainty. Figures 5c - 5e present three representative individual realizations (#1, #30, and #54). In these realizations, the center of the TSF contains a noticeably higher content of the Fe*density.

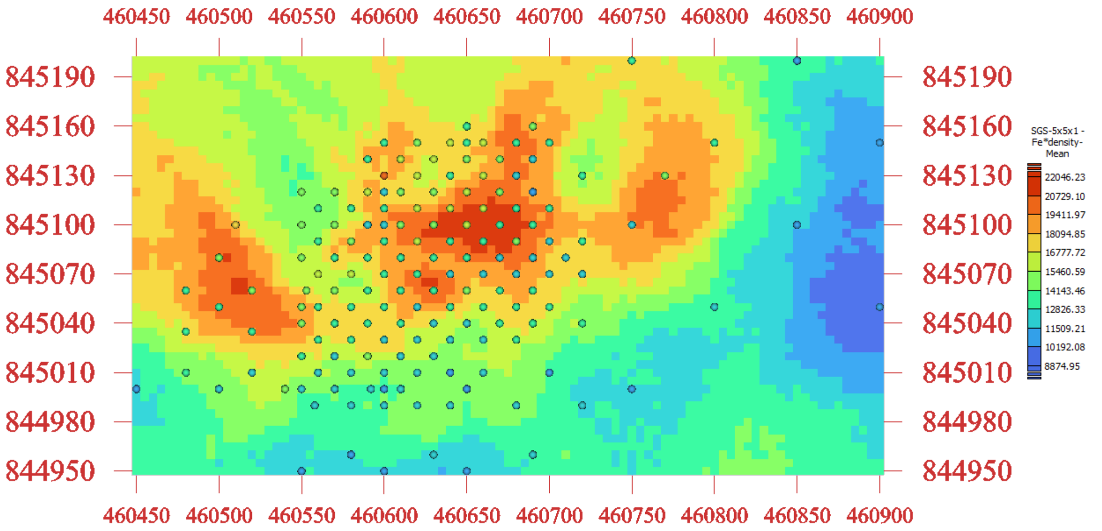


a)

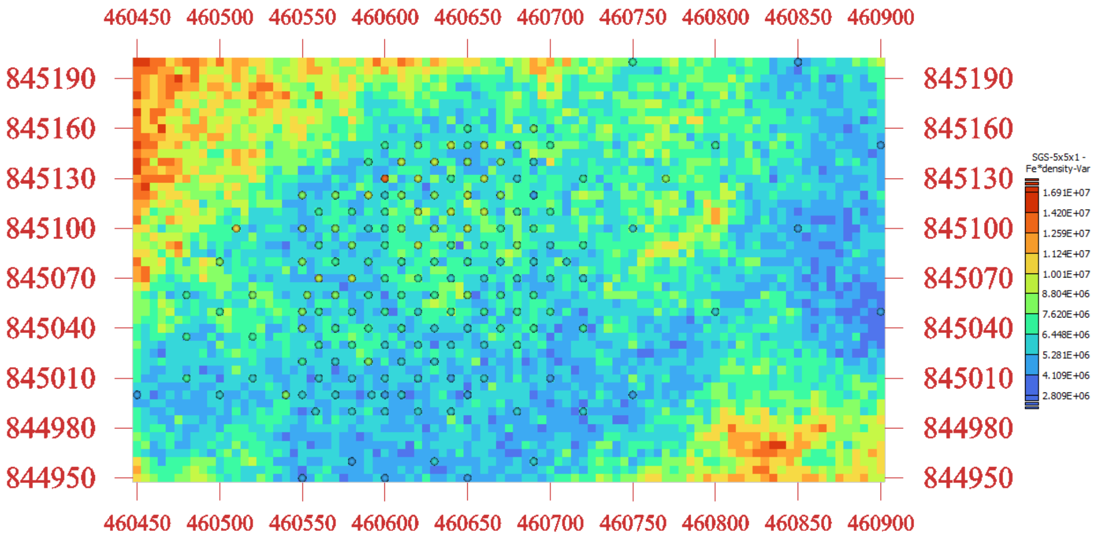


b)

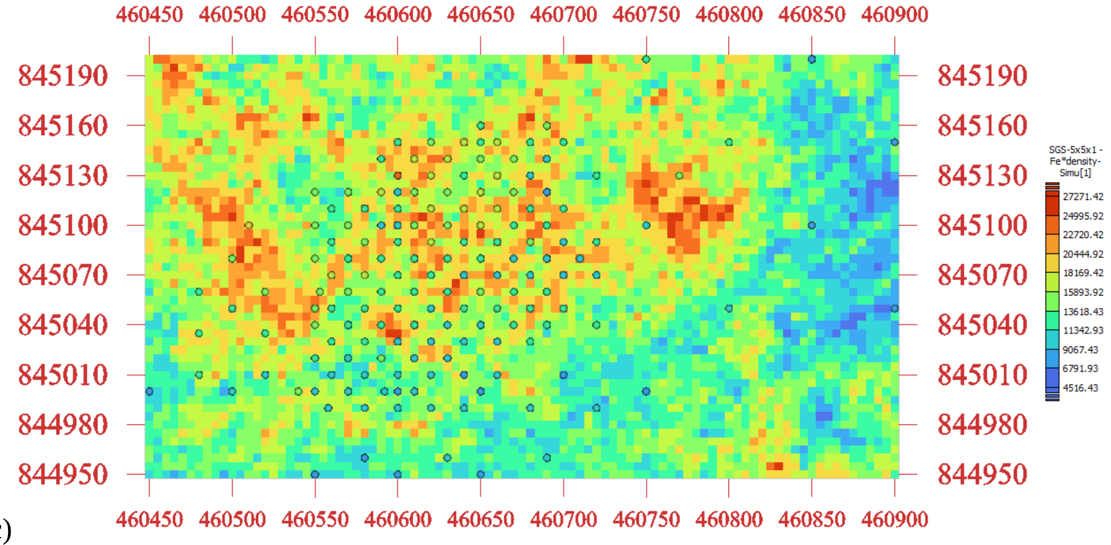


c)

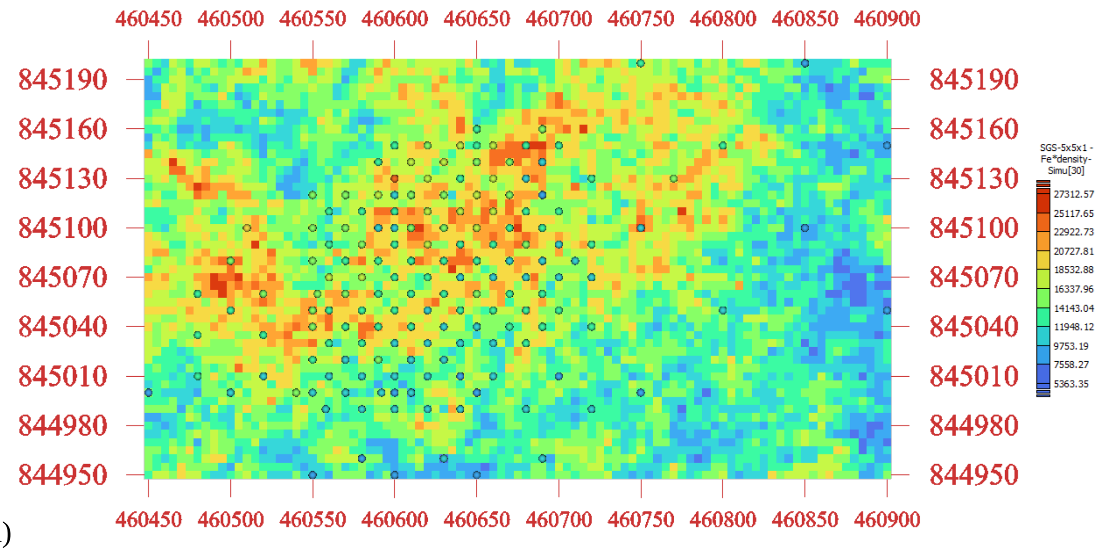


d)

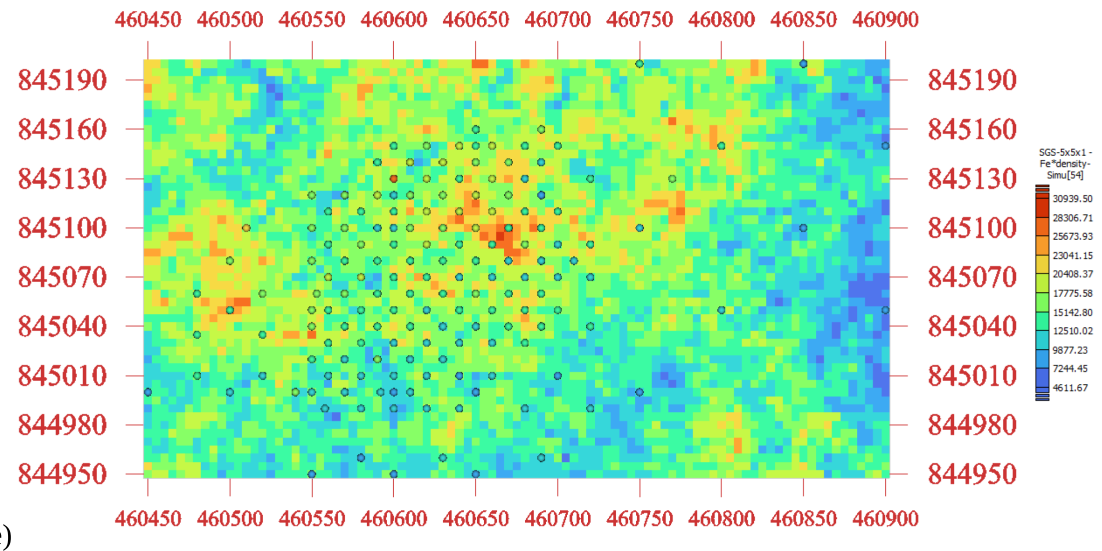


e)

Figure 5. Fe*density simulation on 5x5x1 m grid on a slice 7, a) Mean map, b) Variance map, c) Realization #1, d) Realization #30, e) Realization #54

Figure 6 represents the outcomes of the co-simulation of a Normalized density over a 5x5x1m grid. Figure 6a provides the mean map for normalized density, reflecting a spatial trend of normalized density across the TSF. Denser material appears in deeper and central zones, which is consistent with expected stratification during the deposition of a TSF. Figure 6b represents a variance in the simulated in normalized density, the variance was observaly increased in boundaries and under-sampled regions. Figures 6c - 6e present three realizations of normalized density: #1, #30, #54.  These realizations reflect the trend observed in 6a, with a higher concentration of density in central areas of TSF.

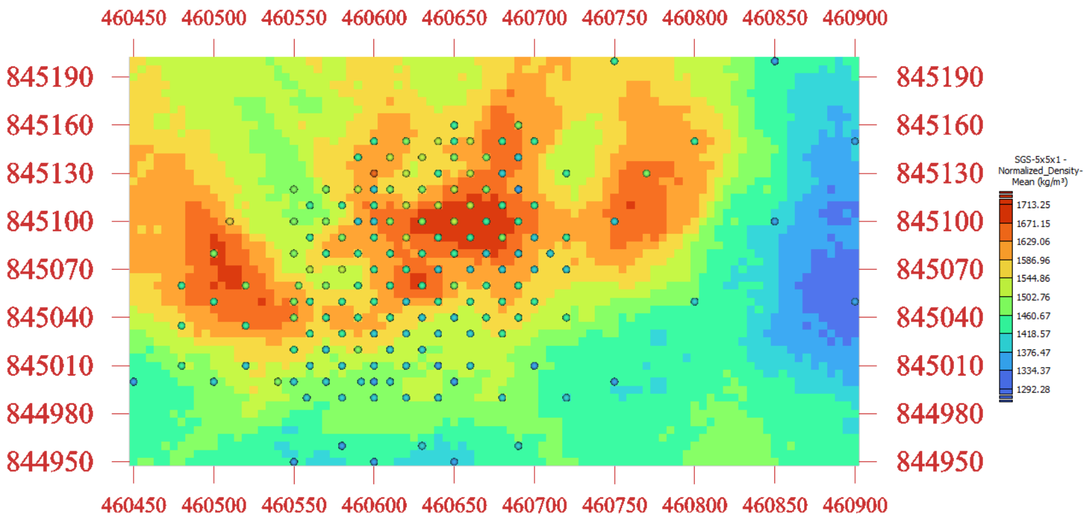


a)

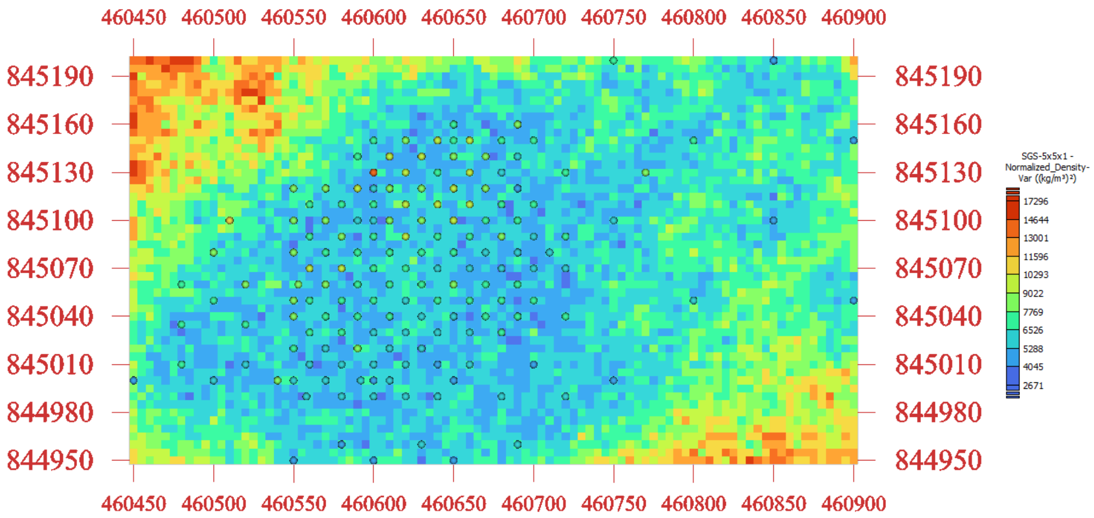


b)

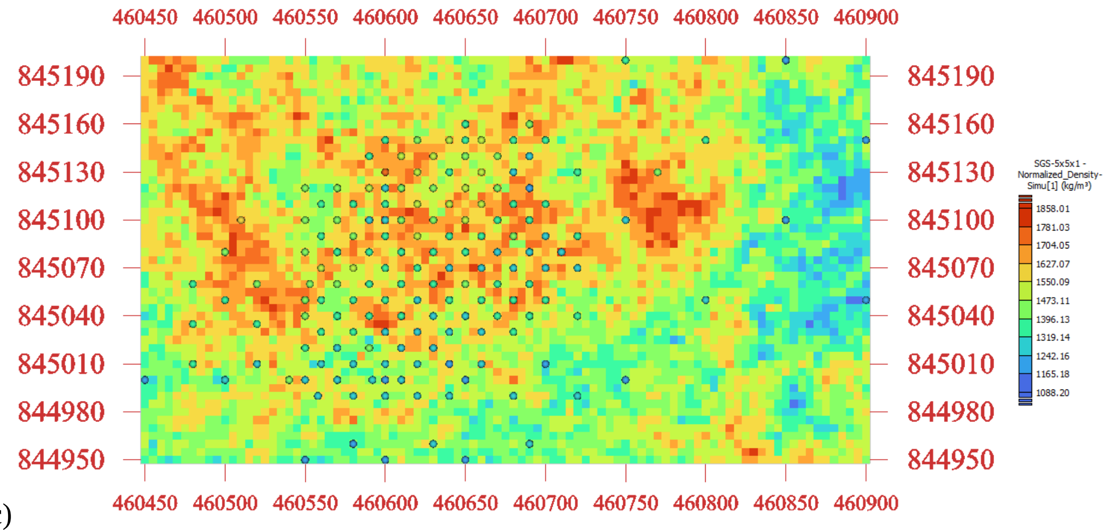


c)

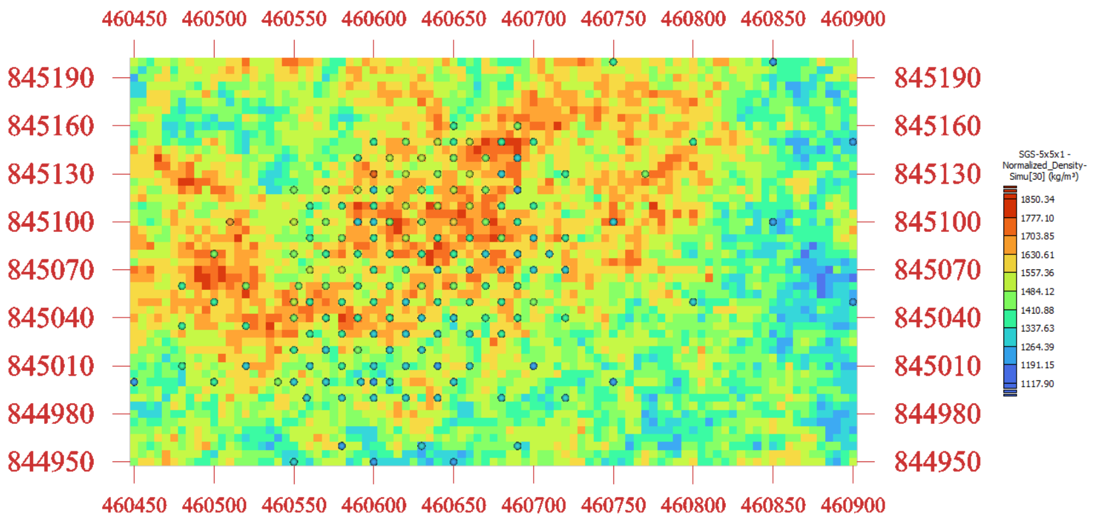


d)

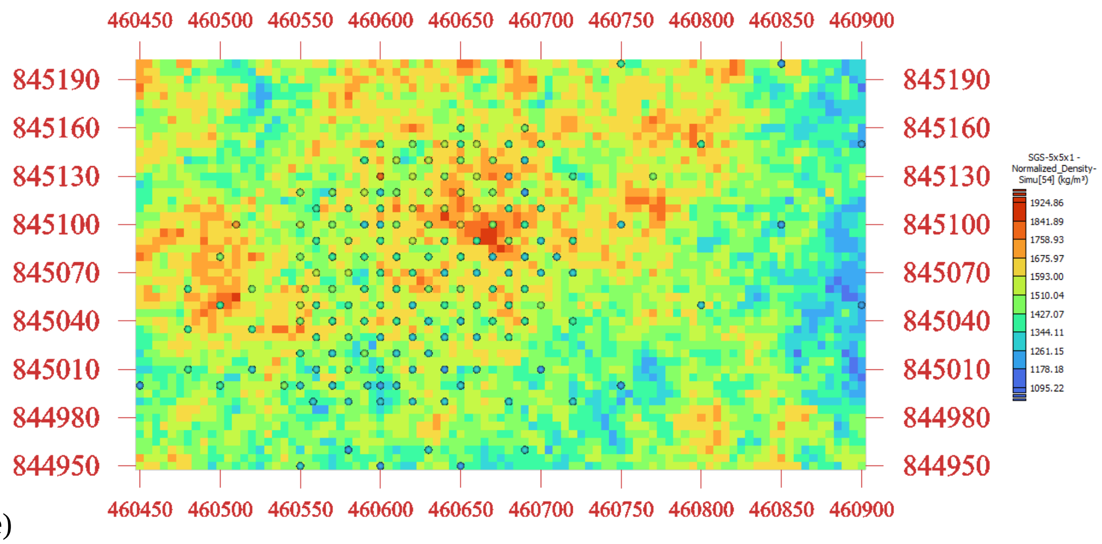


e)

Figure 6. Normalized density simulation on 5x5x1 m grid on a slice 7, a) Mean map, b) Variance map, c) Realization #1, d) Realization #30, e) Realization #54

Figure 7, present SGCS resulting models of the Fe*density over a coarser resolution, 10x10x1m grid. Figure 7a is the mean map of the Fe*density variable, with the preserved spatial trends. Figure 7b shows the variance, which is slightly elevated compared to the 5x5x1 grid. In figures 7c - 7e, the three realizations #1, #30, #54, illustrating various possible scenarios. The trend of the increased values of Fe*density in the central areas of the tailings storage is maintained.

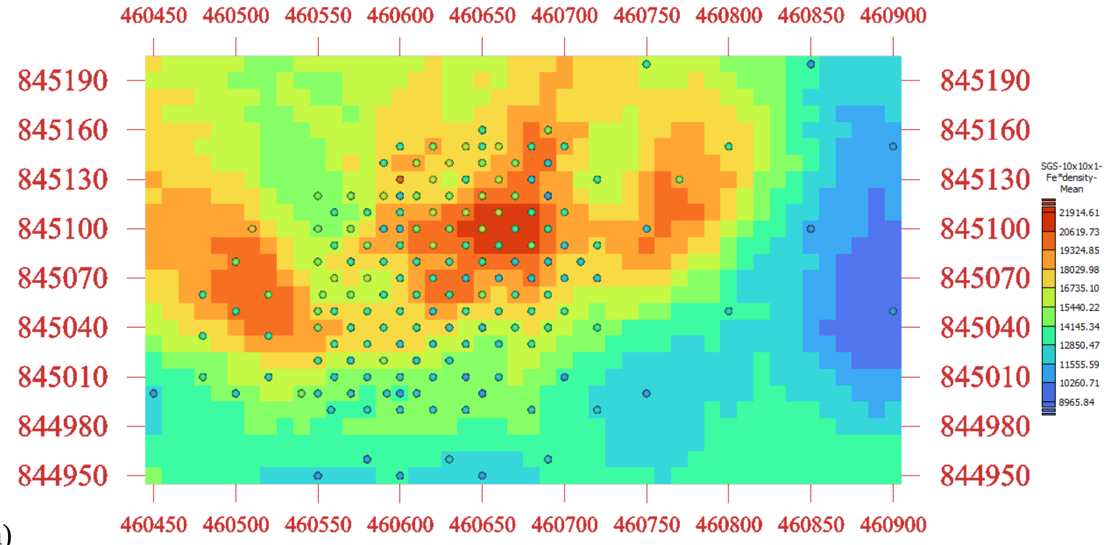


a)

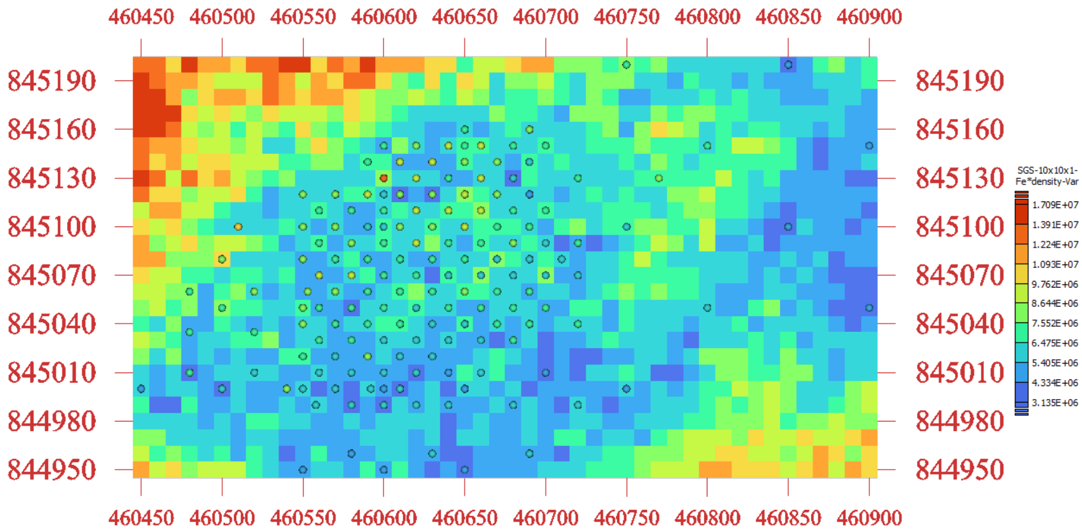


b)

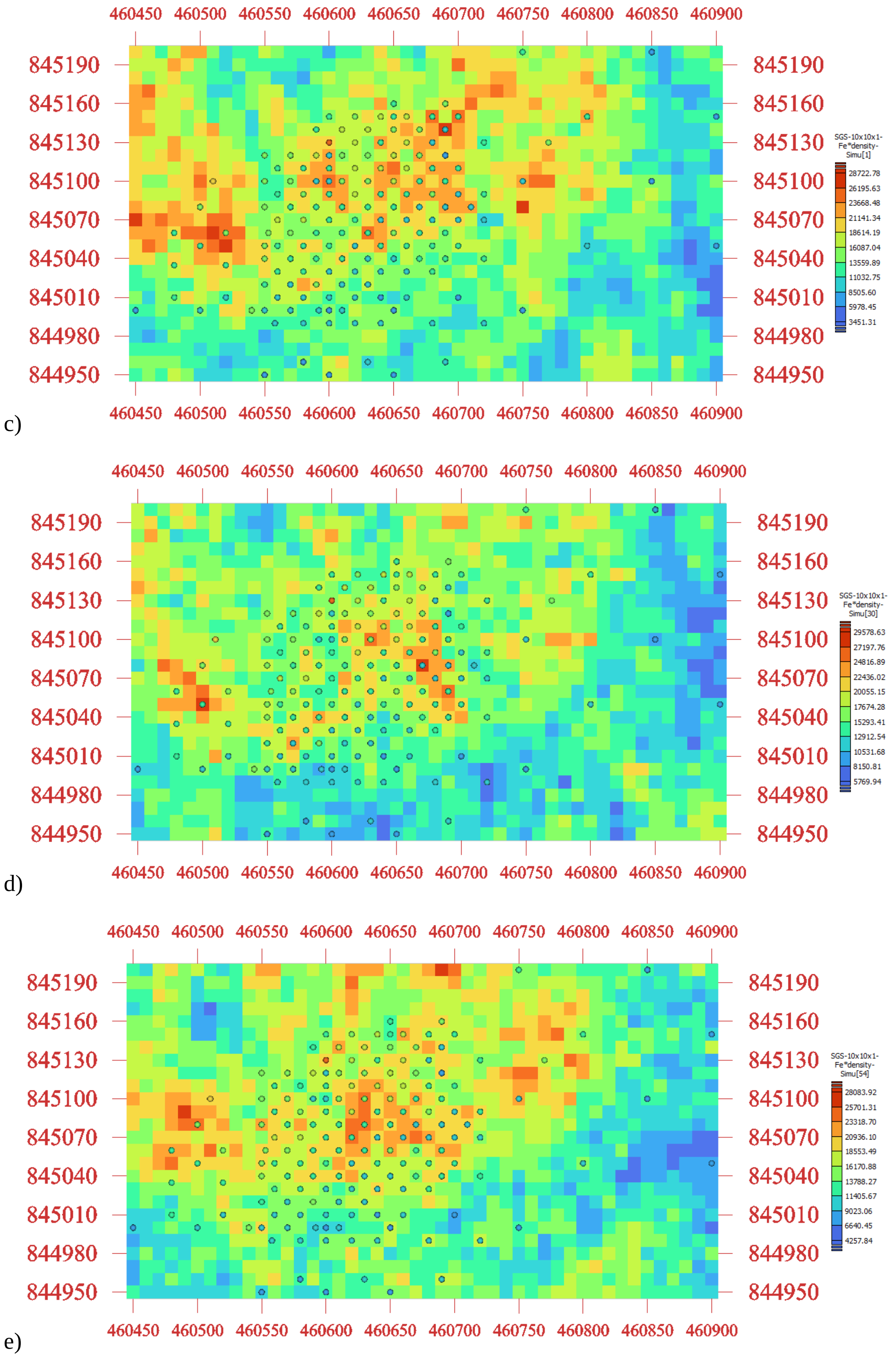


Figure 7. Fe*density simulation on 10x10x1 m grid on a slice 7, a) Mean map, b) Variance map, c) Realization #1, d) Realization #30, e) Realization #54

Figure 8 shows the outcomes of the Normalized density of the SGCS over a 10x10x1m grid. Figures 8a shows mean normalized density from all 100 realizations. Figure 8b shows the corresponding variance map, highlighting uncertainty in coarser grid blocks. Figurec 8c - 8e are the three sample realizations, #1, #30, #54. All the maps show the same trends that were observed in the previous simulations.

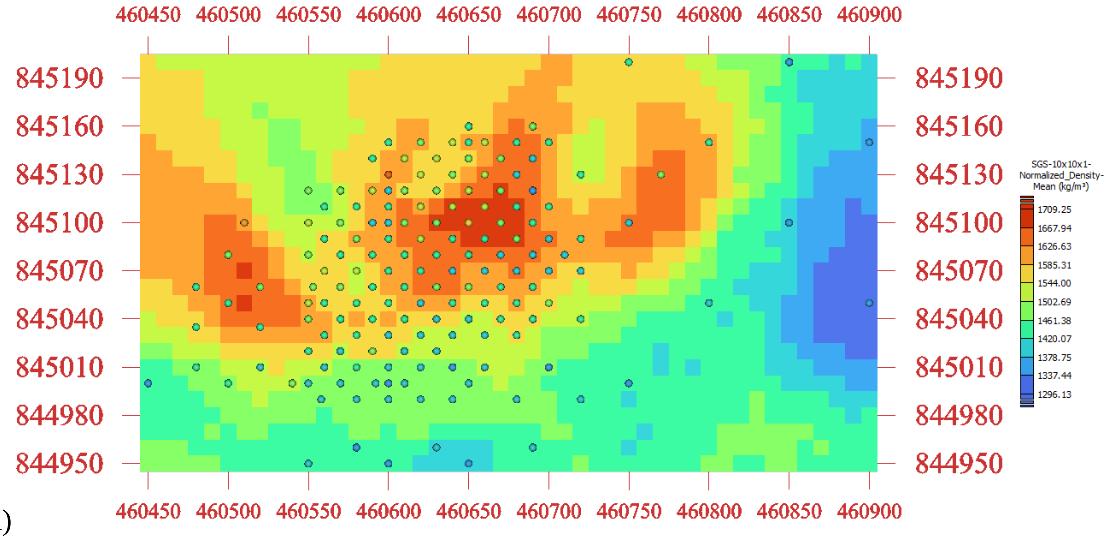


a)

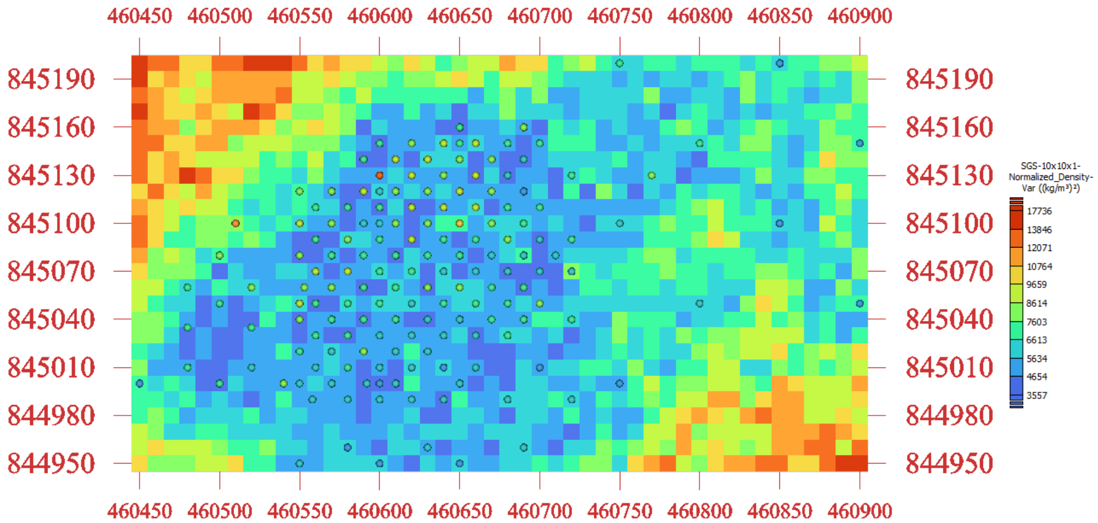


b)

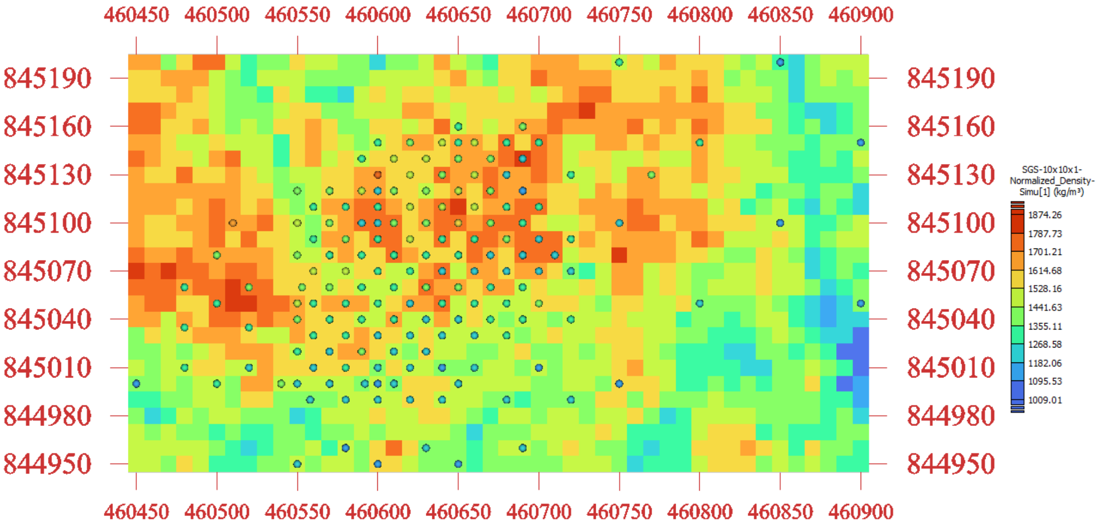


c)

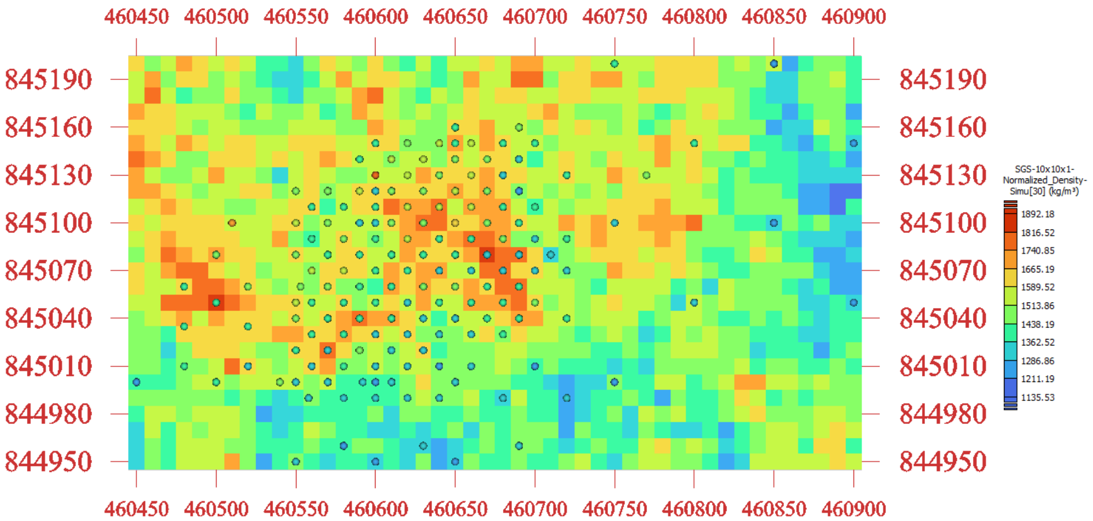


d)

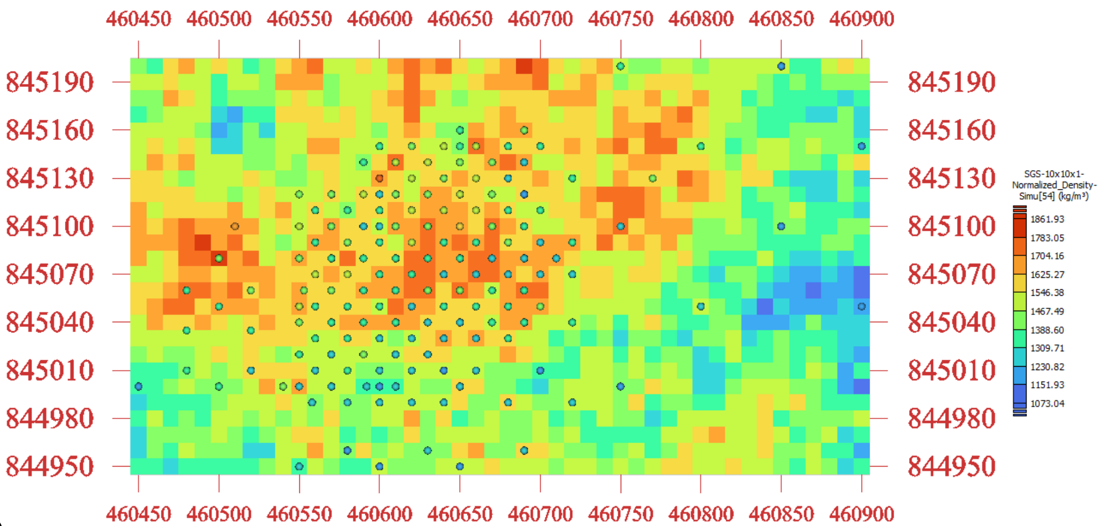


e)

Figure 8. Normalized density simulation on 10x10x1 m grid on a slice 7, a) Mean map, b) Variance map, c) Realization #1, d) Realization #30, e) Realization #54

By generating simulations for both Fe*density and normalized density, it becane possible ti estimate the realizations, mean (E-type)m and variance for the Iron grade. The mean maps (Figures 9a, 10a), and individual realizations (Figures 9c - 9e, and 10c - 10e) are obtained by applying the inversed equation 10, which involves dividing the simulated Fe*density by the simulated Normalized density. The variance maps of Fe grade (Figures 9b and 10b) was then calculated based on the variability of 100 realizations.

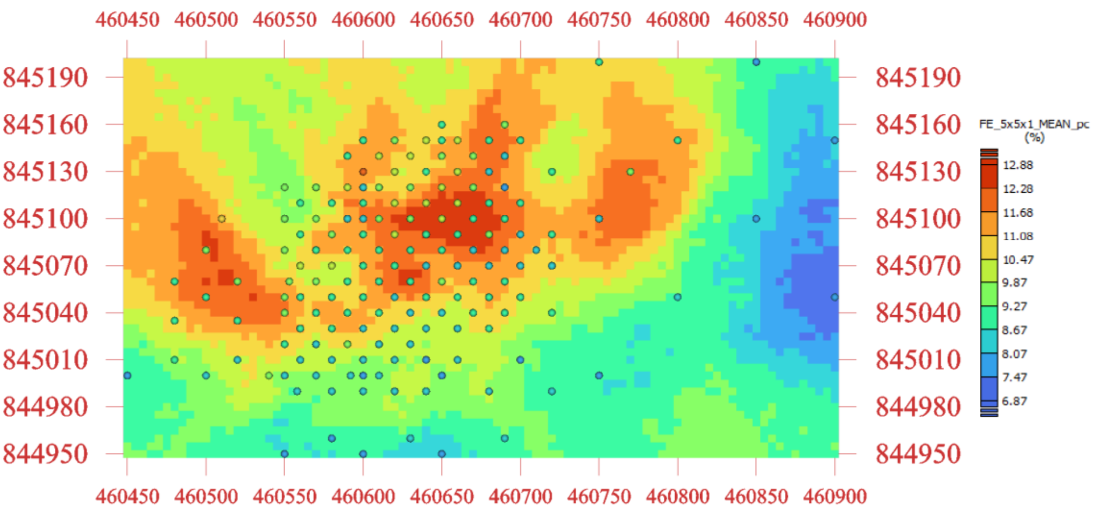


a)

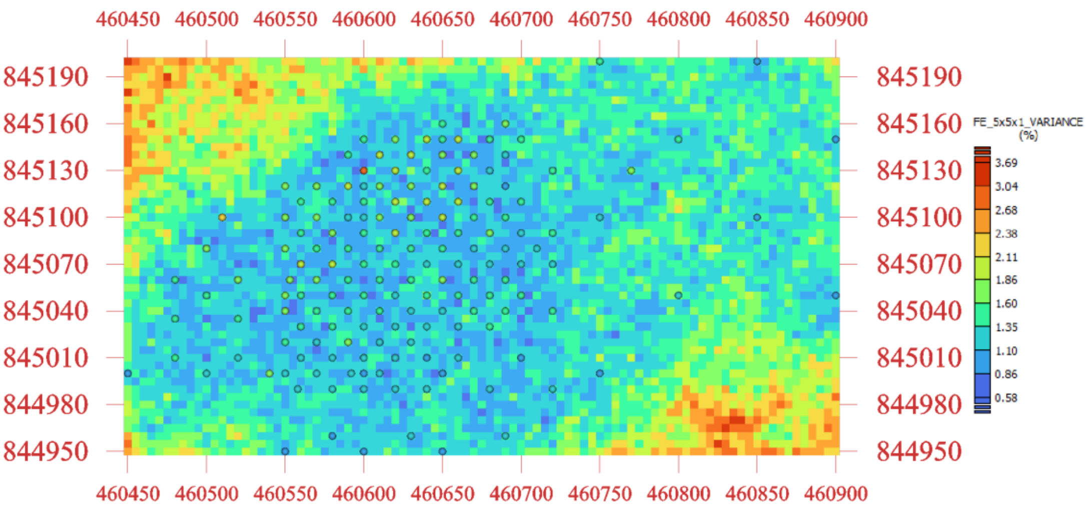


b)

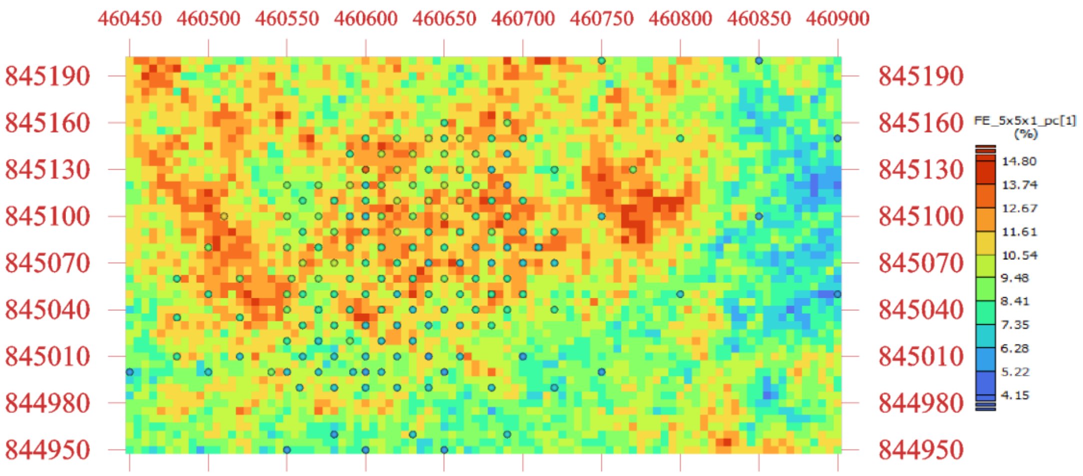


c)

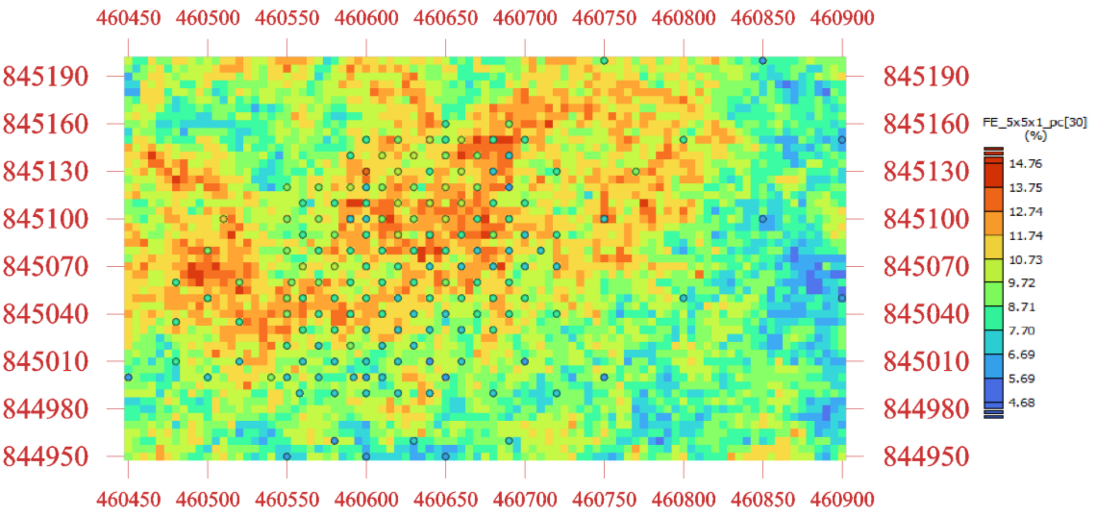


d)

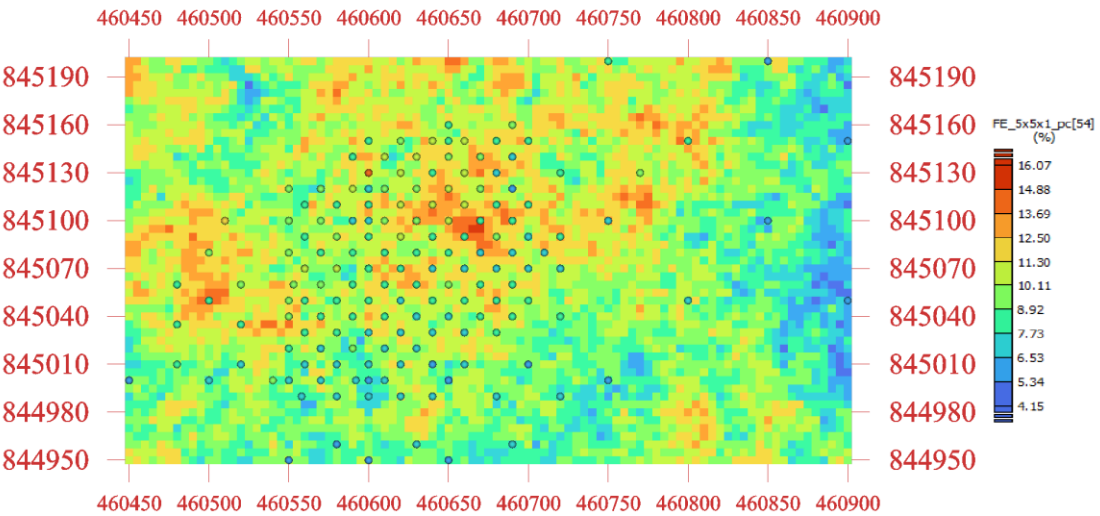


e)

Figure 9. Simulated Fe simulation on 5x5x1 m grid on a slice 7, a) Mean map, b) Variance map, c) Realization #1, d) Realization #30, e) Realization #54

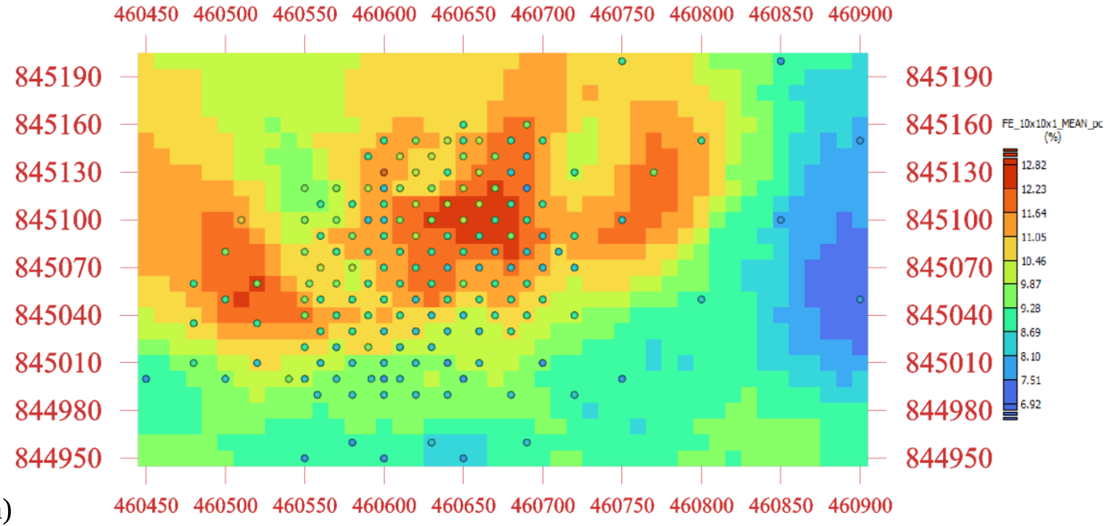
460450 460500 460550 460600 460650 460700 460750 460800 460850 460900
845190
845160
845130
845100
845070
845040
845010
844980
844950
FE_10x10x1_MEAN_pc
(%)
12.82
12.23
11.64
11.05
10.46
9.87
9.28
8.69
8.10
7.51
6.92
a)

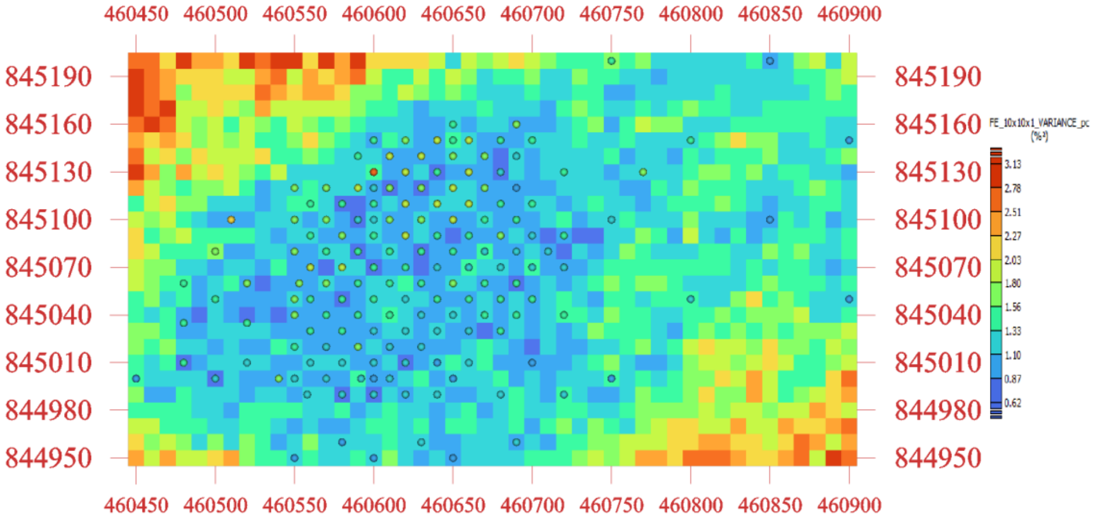
460450 460500 460550 460600 460650 460700 460750 460800 460850 460900
845190
845160
845130
845100
845070
845040
845010
844980
844950
FE_10x10x1_VARIANCE_pc
(%²)
3.13
2.78
2.51
2.27
2.03
1.80
1.56
1.33
1.10
0.87
0.62
b)

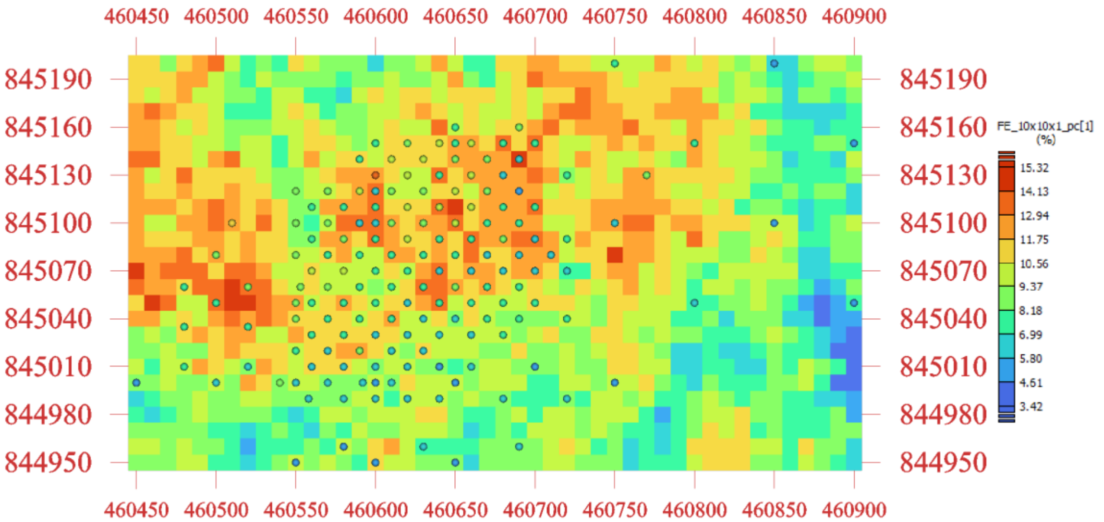
460450 460500 460550 460600 460650 460700 460750 460800 460850 460900
845190
845160
845130
845100
845070
845040
845010
844980
844950
FE_10x10x1_pc[1]
(%)
15.32
14.13
12.94
11.75
10.56
9.37
8.18
6.99
5.80
4.61
3.42
c)

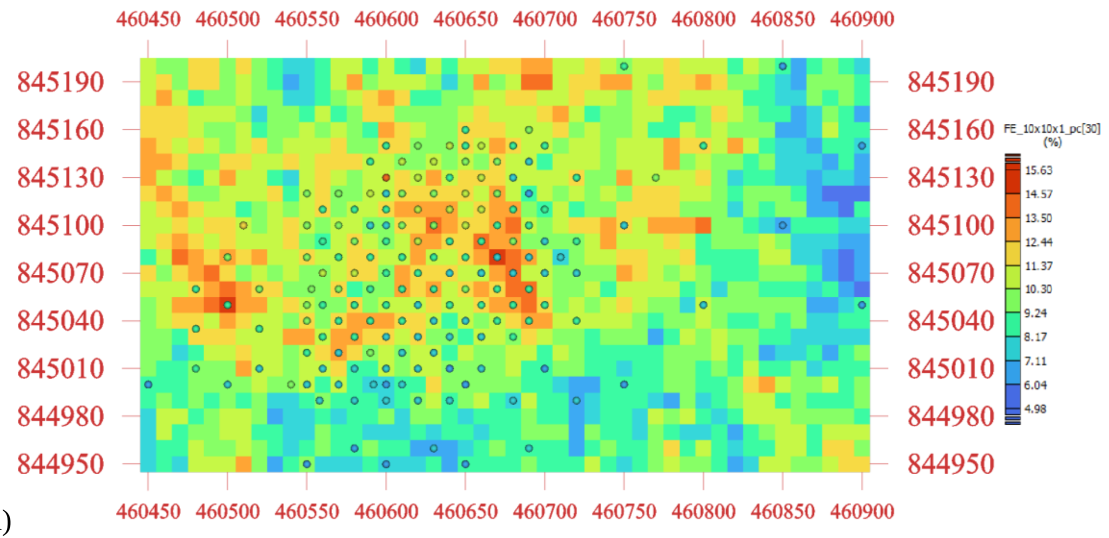


d)

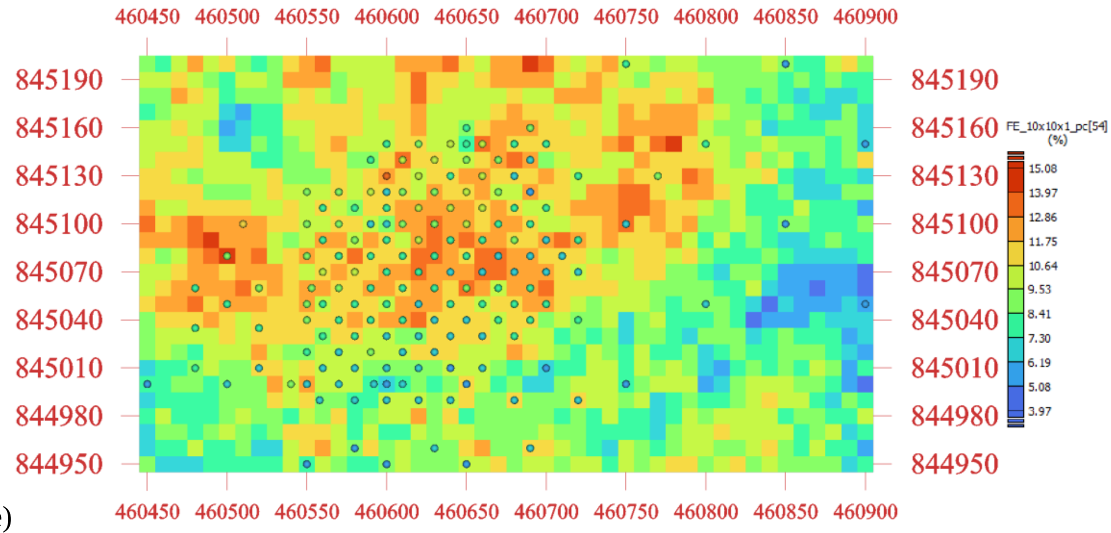


e)

Figure 10. Simulated Fe on 10x10x1 m grid on a slice 7, a) Mean map, b) Variance map, c) Realization #1, d) Realization #30, e) Realization #54

Table 4. Statistical parameters comparison of sampled iron grade with the SGCS results from both grids

| | Original values of iron grade from sampling | Iron grade values from all 100 realizations of SGCS over 5x5x1 grid | Iron grade values from all 100 realizations of SGCS over 10x10x1 grid |
|---|---|---|---|
| Mean value (%) | 10.02 | 9.46 | 9.44 |
| Variance ($\%^2$) | 4.664 | 1.598 | 1.616 |

| | | | |
|---|---|---|---|
| Std. Dev (%) | 2.16 | 1.26 | 1.27 |
| Minimum value (%) | 2.79 | 5.60 | 5.50 |
| Maximum value (%) | 17.01 | 13.40 | 13.36 |

Table 4 presents a statistical comparison between the original sampled Fe grade values and the simulated values obtain through SGCS on both 5x5x1 m and 10x10x1 m grids. The common trend for the SGCS for both of the grids is the smoothing effect, the average grade decreased, together with the range and variance. These changes are also observable in Figures 10a and 10b. Figure 10a shows the histogram of Fe grade values from SGCS over a 5x5x1m, The distribution of the Fe grades is approximately normal, with slightly suppressed extremes. Figure 10b shows the histogram of the Iron grade distribution over a 10x10x1 m grid. In the figure 10b, the Fe grade distribution has a similar distribution to the one in figure 10a, however, the 10x10x1m simulation suffered more extensively from a smoothing effect.

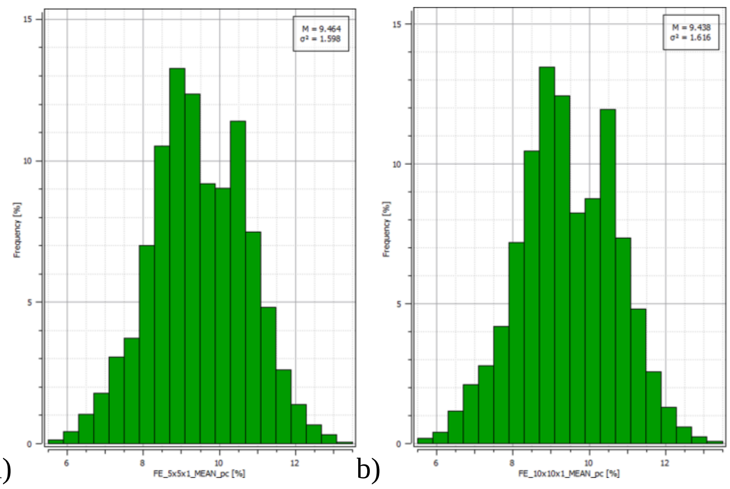


a) b)

Figure 11. Histograms of the iron grade simulated over a)5x5x1 m grid, b)10x10x1 m grid

The figures 12 and 13 show the swath plots of the simulated Iron grade along the east, north, and vertical directions for both 5x5x1 m grid (Figure 12), and 10x10x1 m grid (Figure 13). Figure 12a show the swath plot along the eastern direction of a Fe grade,gradual decreasing trend is observed, with the highest values are concentrated between easting coordinates 460,500 and 460,600 m, whereas in the 10x10x1 m grid simulation of the Fe grade along the east direction (Figure 13a), the eastward decreasing trend seen, however the transitions between zones are smoother and less defined. In the northern direction, the SGCS for the Iron grade over

5x5x1 m grid (Figure 12b) display a moderate variation in Fe grade with slightly higher concentration near the center. Figure 13b, the swath plot of simulated Fe grade over 10x10x1 m grid is consistent along the northing coordinates, however the extreme values appear less frequently when compared with Figure 12b. In vertical direction, swath plot of the simulated Fe grade (Figure 12c), vertical enrichment is observed, with increase of the Fe grade towards the mid-depth. In figure 13c, the vertical swath plot of simulated Fe grade over a 10x10x1m grid, show that Fe increases toward the middle laters, however the variation is less than in the Figure 12c.

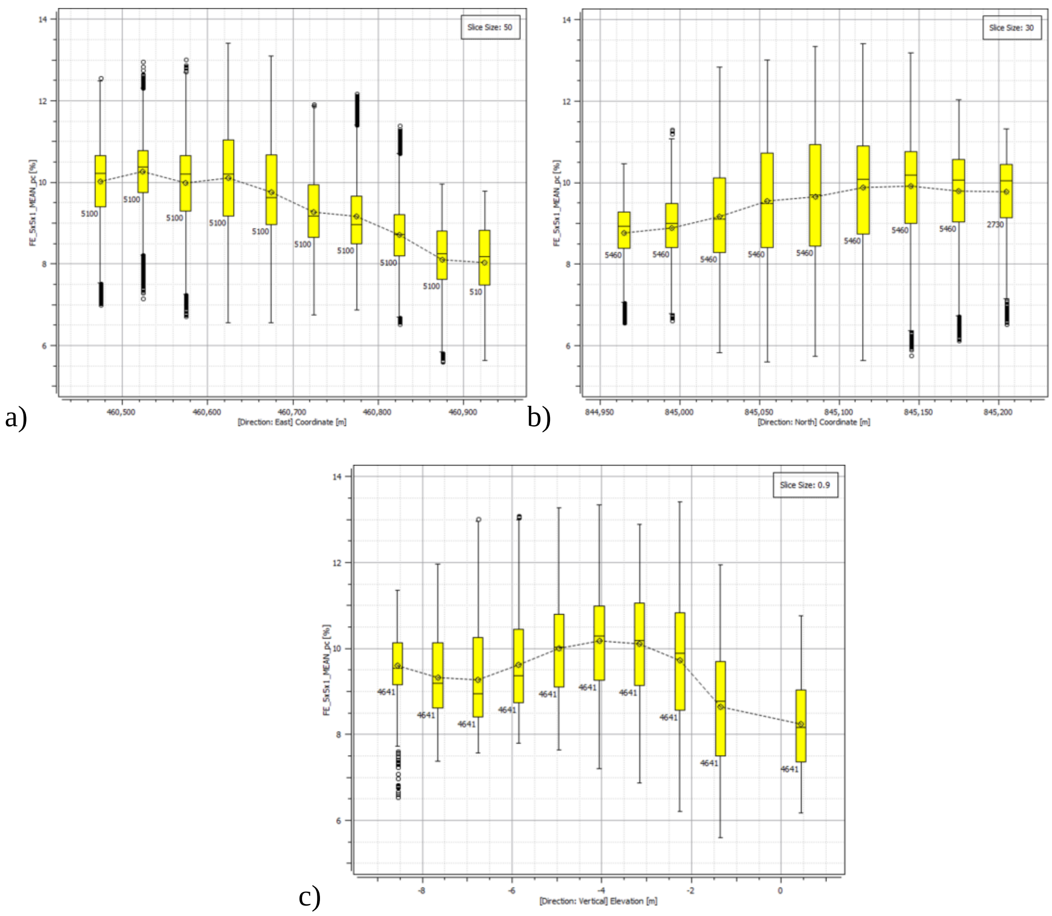


Figure 12. Swath plot of simulated iron grid on 5x5x1 grid, a) East direction, b) North direction, c) Vertical direction

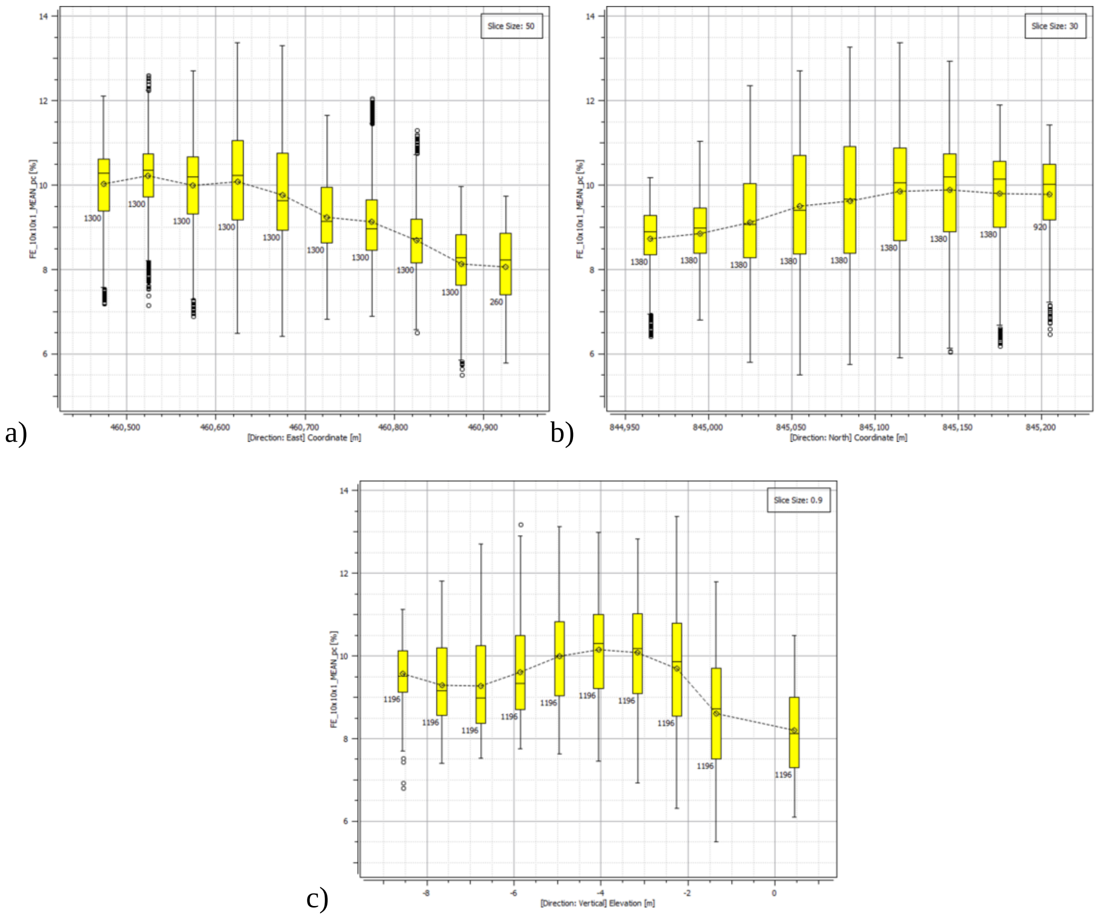


Figure 13. Swath plot of simulated iron grid on 10x10x1 grid, a) East direction, b) North direction, c) Vertical direction

## 4.7 Simulation Validation

It is essential to conduct a validation over the obtained simulations for the iron grade. Its principle is based on the comparison of experimental variograms, histograms, and swath plots of the obtained Fe realizations with the sampled values of the Fe. The first step is to obtain the experimental variogram for the sampled Fe values. The variogram consisted of horizontal and vertical directions. The horizontal variogram was constructed based on the Lag value of 11.2 m and, Maximum distance of 319.2 m. Obtained variogram is seen in the Figure 14.

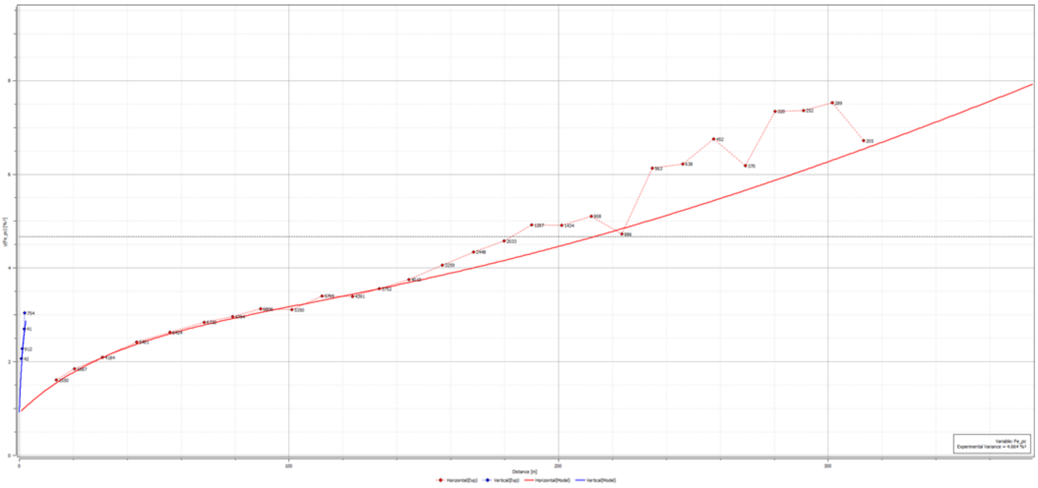

Figure 14. Experimental Variogram of Sampled Fe

Further on, the simulation of the Fe for both of the grids were compared with the sampled data by the key geostatistical tools. Figure 15 present comparison of the histograms of the simulated Iron grade over 5x5x1 m grid (Figure 15a), and 10x10x1 m grid (Figure 15b) with the original sampled Iron grade histogram. Figures 16 and 17 compares the variogram of the simulated Iron grade over 5x5x1 m grid and 10x10x1 m grid respectively with the variogram of the sampled Fe grade, along the east direction (Figures 16a and 17a), north direction (Figures 16b and 17b), vertical direction (Figures 16c and 17c). Figures 18 and 19 present a simulation validation by comparing the swath plots of the obtained simulated Iron grades over 5x5x1 m grid (Figure 18) and 10x10x1 m grid (Figure 19), along the east direction (18a and 19a), north direction (18b and 19b), and vertical direction(18c and 19c).

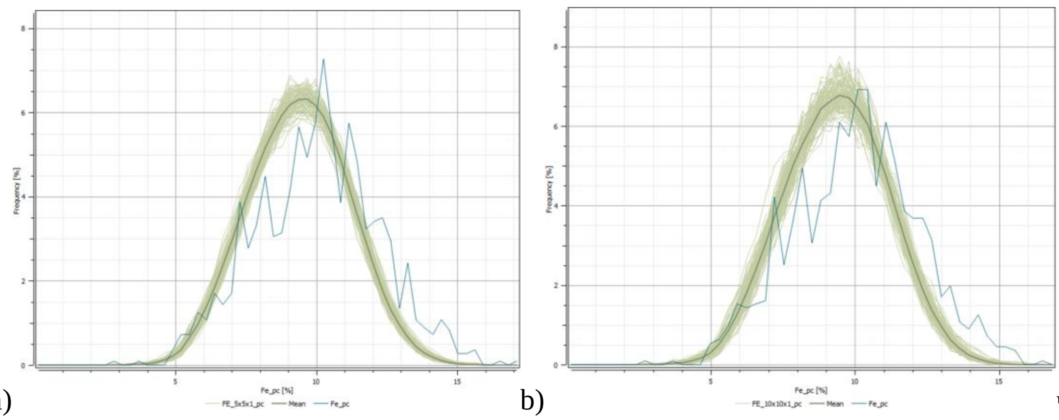

a) b) ч

Figure 15. Validation of histograms of SGCS with the sampled Iron grade values, a) SGCS over 5x5x1 m grid, b) 10x10x1 m grid

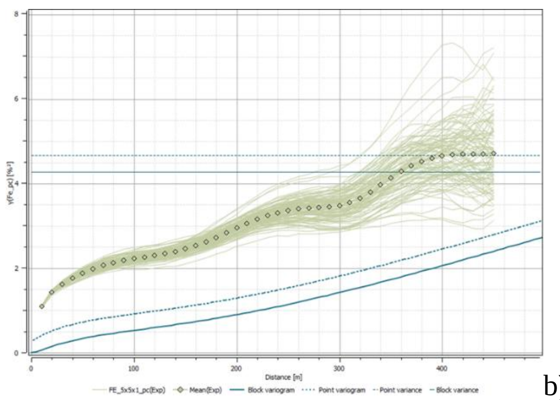

a)

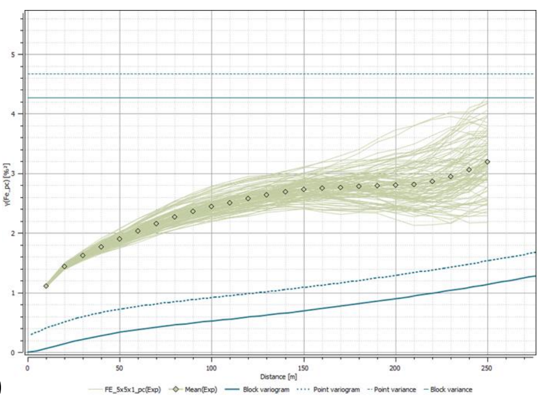

b)

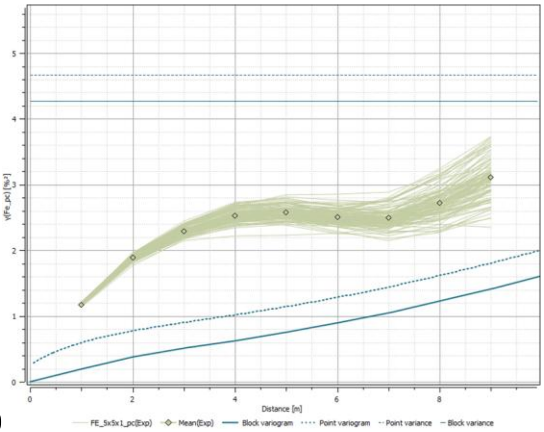

c)

Figure 16. Validation of variograms of SGCS over 5x5x1 m grid with the sampled iron grade variogram, a) East direction variogram, b) North direction variogram, c) vertical direction variogram

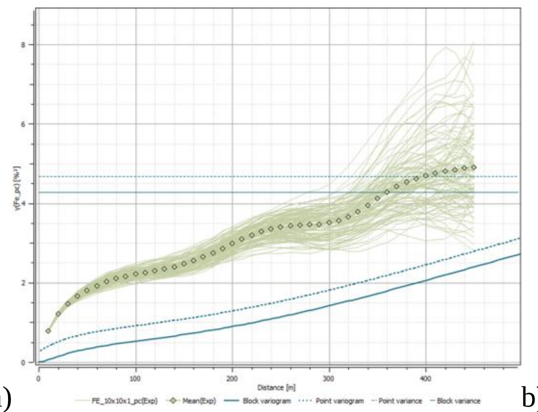

a)

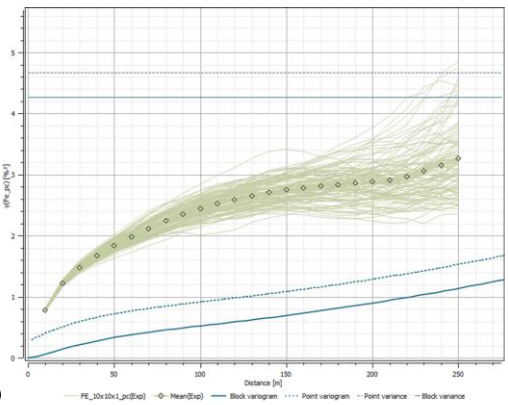

b)

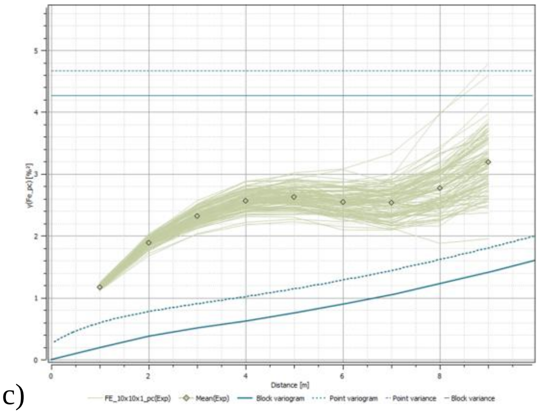


c)

Figure 17. Validation of variograms of SGCS over 10x10x1 m grid with the sampled iron grade variogram, a) East direction variogram, b) North direction variogram, c) vertical direction variogram

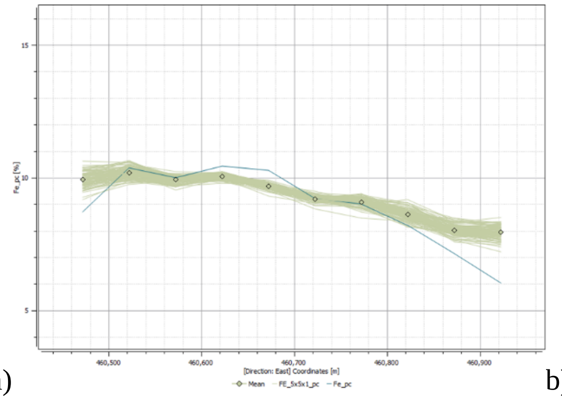


a)

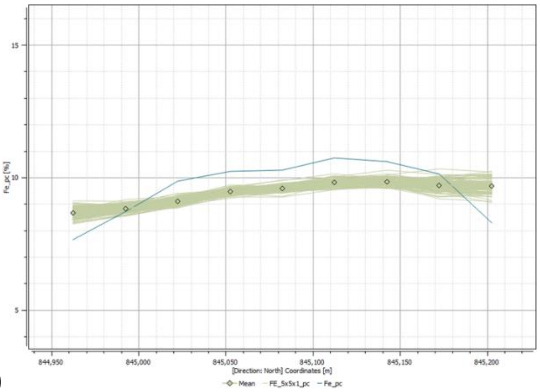


b)

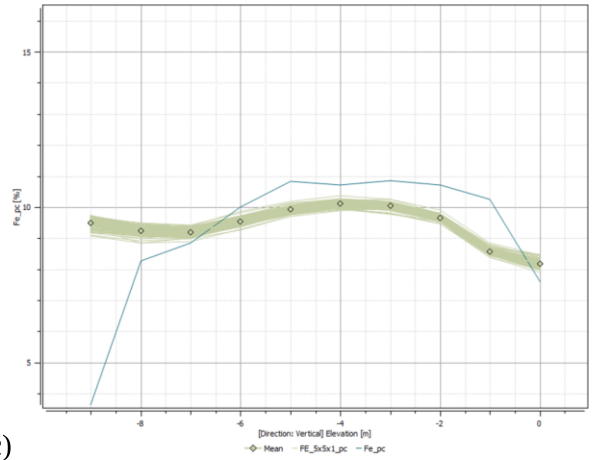


c)

Figure 18. Validation of swath plots of SGCS over 5x5x1 m grid with the sampled iron grade swath plot, a) East direction, b) North direction, c) vertical direction

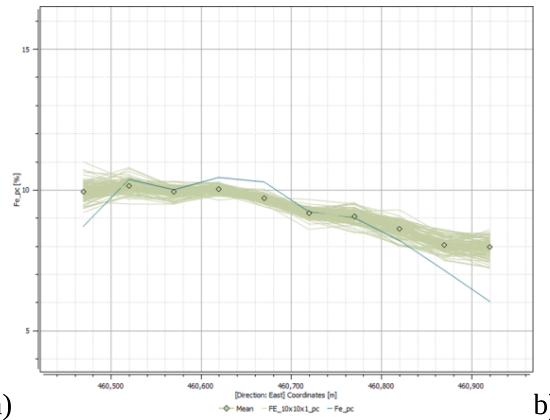

a)

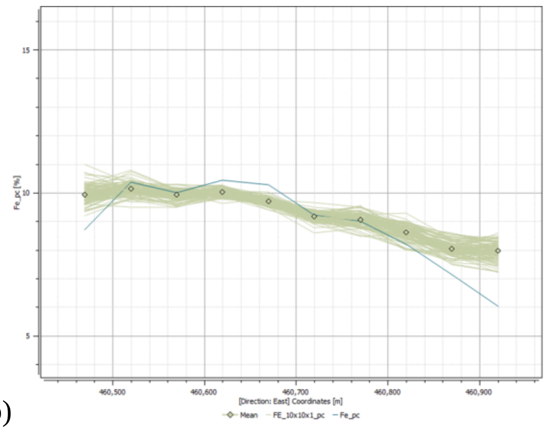

b)

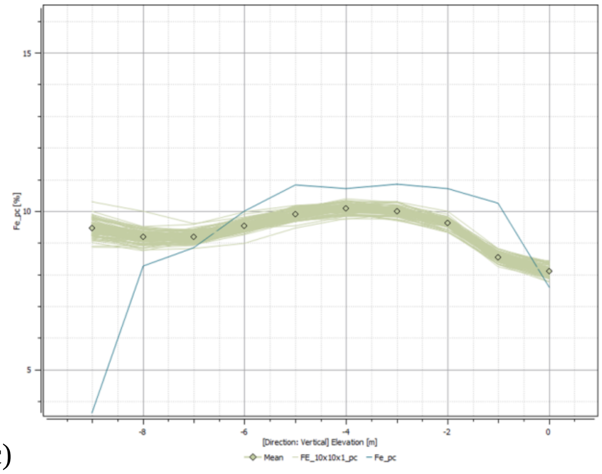

c)

Figure 19. Validation of swath plots of SGCS over 10x10x1 m grid with the sampled iron grade swath plot, a) East direction, b) North direction, c) vertical direction

## 4.8 Grade Tonnage Estimations

For a further evaluation of the SGCS results, grade tonnage analysis is performed for both 5x5x1 m and 10x10x1 m simulation grids. This analysis provides essential insights into the amount of recoverable metal at various cutoff grades and is critical step to assess the economic viability of any mining project. The metal recovery was assumed to be 80%, and the mean density variable, which was obtained as a result of a SGCS.

Figure 20 and 21 represents grade tonnage tables and curves results from the SGCS over a 5x5x1 m and 10x10x1 m grids respectively. Figure 20a and 21 a is a Grade Tonnage Table, which presents numerical results from the SGCS, they provide values for cutoff grades (%), Tonnage (kg), Contained metal (kg), Mean Fe grade (%), Volume ($m^3$), and Benefit (kg) which refers to recoverable material. Figures 20b and 21b show a plot, with two contrasting trends, decrease of tonnage and mean grade increase as the cutoff increases. Figures 20c and 21c Shows Metal quantity against the Cutoff Grade. This curve illustrates the total content of Fe metal as a function of cutoff, A cutoff increases, as metal content decreases. Figures 20d and 21d is a Metal Quantity vs Tonnage curve, which demonstrates relationship between contained metal with total tonnage. Figures 20e and 21e, is a plot of BEnefit vs Cutoff Grade. As the cutoff grade increases, the benefit decreases, an plot allows to determine a cuttof with a maximized net benefit. Figures 20f and 21f show a plot of Volume against the Cutoff Grade, Volume decreases as the Cutoff grade increases.

| Cutoff [%] | Tonnage [kg] | Metal [kg] | Grade [%] | Volume [$m^3$] | Benefit [kg] |
|---|---|---|---|---|---|
| **2.77** | 1,364,539,136.00 | 129,191,120.00 | 9.47 | 928,198 | 91,428,576.00 |
| **4.77** | 1,361,365,120.00 | 129,054,096.00 | 9.48 | 925,743 | 64,152,084.00 |
| **6.77** | 1,271,251,840.00 | 123,514,312.00 | 9.72 | 859,274 | 37,483,344.00 |
| **8.77** | 885,049,344.00 | 92,969,184.00 | 10.50 | 586,828 | 15,373,178.00 |
| **10.77** | 328,133,376.00 | 38,658,428.00 | 11.78 | 210,953 | 3,326,925.25 |
| **12.77** | 41,806,980.00 | 5,599,858.00 | 13.39 | 26,152 | 262,184.34 |
| **14.77** | 1,125,098.13 | 170,607.88 | 15.14 | 698 | 4,459.90 |
| **16.56** | 6,934.52 | 1,160.71 | 16.73 | 4 | 12.43 |

a)

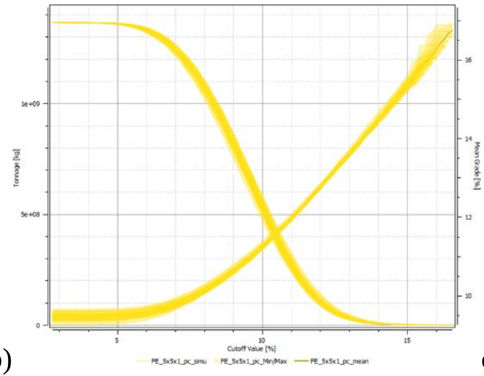

b)

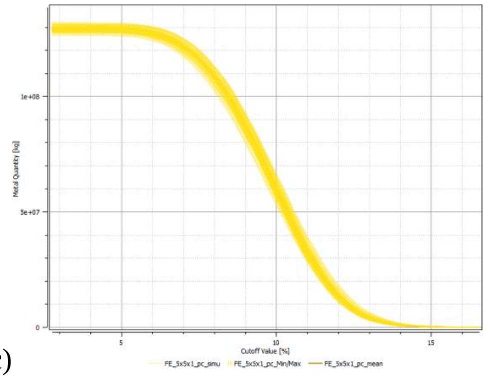

c)

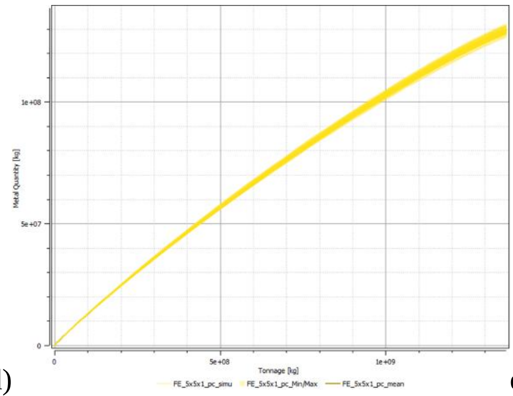

d)

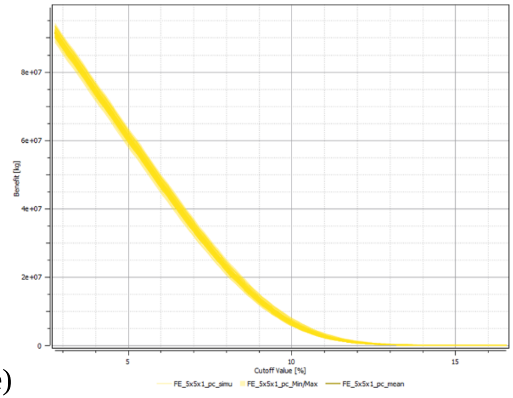

e)

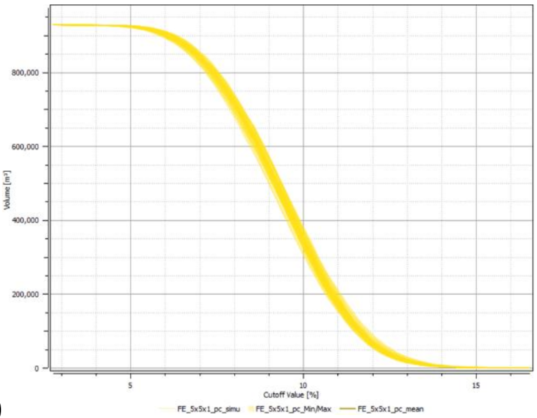


f)

Figure 20. 5x5x1 m grid Fe Grade Tonnage  a)Tables, b) Tonnage and Mean Grade (Cutoff), c) Metal Quantity (Cutoff), d)Metal Quantity (Tonnage), e) Benefit (Cutoff), f) Volume (Cutoff)

a)

| Cutoff [%] | Tonnage [kg] | Metal [kg] | Grade [%] | Volume [m³] | Benefit [kg] |
|---|---|---|---|---|---|
| **3.42** | 1,404,539,904.00 | 132,616,584.00 | 9.44 | 956,695 | 84,574,448.00 |
| **5.42** | 1,390,970,880.00 | 131,946,976.00 | 9.49 | 946,349 | 56,549,552.00 |
| **7.42** | 1,209,451,136.00 | 119,789,528.00 | 9.90 | 814,328 | 30,042,340.00 |
| **9.42** | 715,447,168.00 | 77,769,184.00 | 10.87 | 470,298 | 10,370,561.00 |
| **11.42** | 195,170,480.00 | 23,960,820.00 | 12.27 | 124,396 | 1,671,397.88 |
| **13.42** | 15,607,780.00 | 2,177,484.25 | 13.94 | 9,747 | 82,843.76 |
| **15.42** | 190,691.78 | 30,004.43 | 15.74 | 119 | 598.82 |
| **16.22** | 6,581.04 | 1,079.99 | 16.43 | 4 | 12.64 |

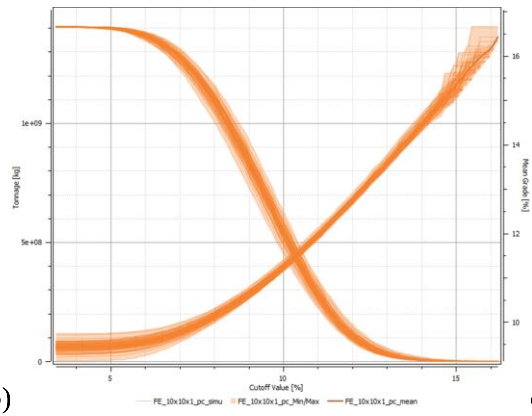

b)

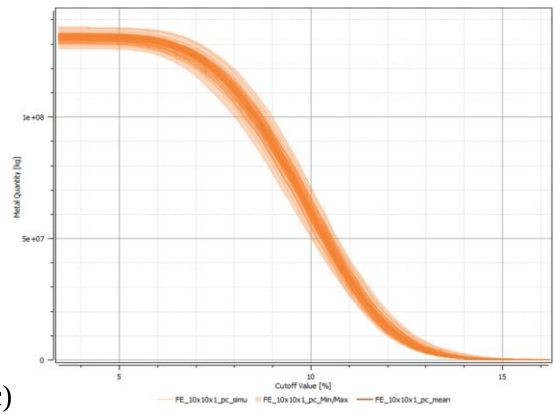

c)

d)

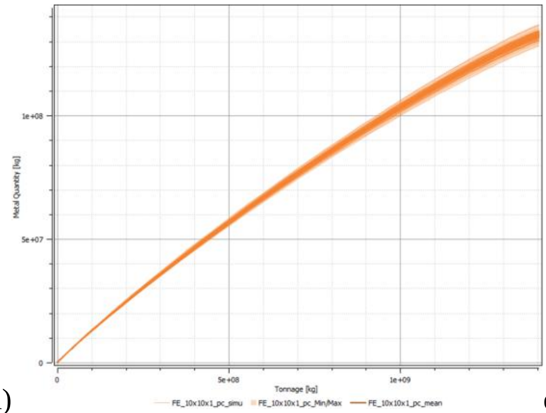


e)

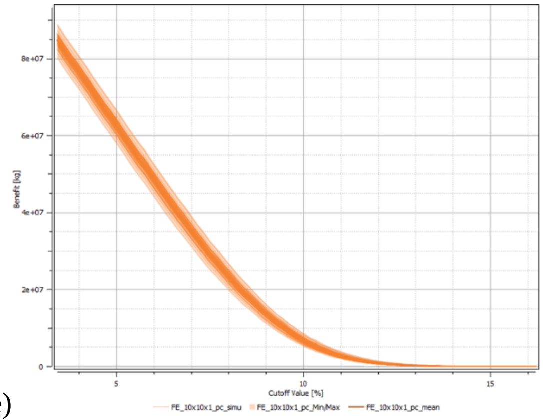


f)

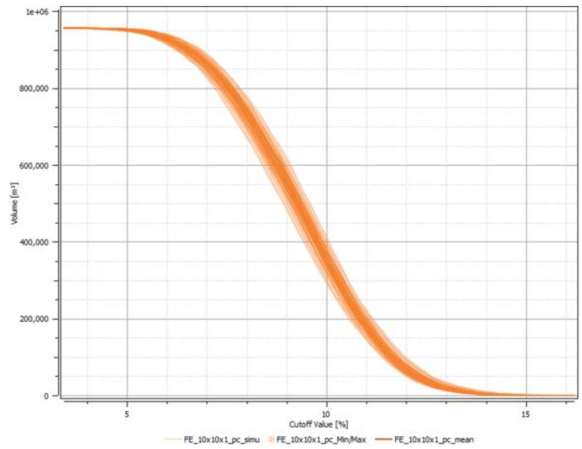


Figure 21. 10x10x1 m grid Fe Grade Tonnage a)Tables, b) Tonnage and Mean Grade (Cutoff), c) Metal Quantity (Cutoff), d)Metal Quantity (Tonnage), e) Benefit (Cutoff), f) Volume (Cutoff)

# 5. DISCUSSION

This study applied Sequential Gaussian Co-Simulation (SGCS) with block support to model the spatial distribution of iron (Fe) grade in a tailings storage facility (TSF) at the Haveri Au-Cu site. The primary goal was to address the challenges associated with modeling non-additive variables in a geologically heterogeneous environment. The processing methods and deposition techniques used during the long mine operation time have caused the inherent heterogeneity, which leads to the complex and non-stationary distribution of the waste within the tailings (Blannin et al., 2023). To mitigate these issues, in addition to the SGCS methodology, the block support system was implemented, which would solve the small-scale variability with a better capture of the spatial distribution of the iron grade. The SGCS was conducted over 2 various grids, 5x5x1 m and 10x10x1 m, and the block discretization for both cases was 5x5x1 m.

## 5.1 Histogram Analysis of Simulated Iron Grade

The histogram analysis is a key tool used to assess and verify the extent to which the statistical parameters and distribution of the SGCS realizations are preserved. This step is essential in simulation-based geostatistics, as maintaining the original histogram ensures that the simulated values accurately reflect the central tendencies and spread of the observed data (Goovaerts, 1997; Rossi & Deutsch, 2014). Based on Figures 2a, 11, and 16, as well as Table 4, the simulations for both grid sizes demonstrated a strong alignment with the original dataset, particularly in terms of the mean and standard deviation. However, a common trend observed in the SGCS realizations was the smoothing effect, which resulted in a narrowing of the value range. Consequently, the maximum and minimum values in the simulations were underrepresented. This smoothing effect likely arises from the averaging nature of block support. As values are estimated across blocks composed of smaller sub-blocks, localized high and low values are averaged out, leading to a dilution of extremes (Goovaerts, 2016). While this may be viewed as a limitation of the block support system, it also enhances the stability and realism of simulation outcomes—an important benefit for practical applications in mine planning. Additionally, the histograms of the simulations revealed the emergence of a secondary population, which may be attributed to the influence of density estimations. Specifically, 192 samples of the 1980 sampling campaign included four additional elements used in density calculation, potentially leading to a slight increase in Fe estimates due to elevated values in the secondary variable. This observation underscores the impact of secondary data quality and variability on co-simulation outcomes and highlights the need for careful validation of auxiliary inputs.

## 5.2 Swath Plot Validation

Swath plots are valuable tools for analyzing the spatial distribution of variables, as they compare the moving averages of simulated and original values, enabling the assessment of consistency across the north, east, and vertical directions. In this study, the swath plots (Figures 2b, 2c, 2d, 12, 13, 18, and 19) demonstrated that the SGCS models effectively preserved the primary spatial trends and gradients of the Fe grade in all three directions. For example, the north-direction swath plots have shown consistent reproduction of large-scale grade variability, highlighting the model's capacity to capture the anisotropic characteristics of the tailings' spatial structure. These visual tools are crucial for identifying zones of higher mineral concentration, which supports more targeted and efficient resource extraction strategies. However, some minor deviations were observed in the vertical swath plots, particularly in the case of the 10x10x1 m block model (Figure 19c). These deviations are likely due to the limited vertical sampling density, which can negatively affect the variogram fitting, reducing the simulation accuracy in the vertical dimension. Additionally, the density variable used as a secondary dataset may not fully reflect vertical variability, further contributing to these deviations. These observations emphasize the need for enhanced vertical data resolution in future tailings modeling efforts to ensure more accurate spatial predictions throughout the entire volume of the storage facility.

## 5.3 Variogram Reproduction

The accurate reproduction of variograms in this study underscores the capability of Sequential Gaussian Co-Simulation (SGCS) to model spatial dependencies and continuity in a geologically complex domain. To ensure that the spatial variability is properly reproduced by the SGCS realization of the observed data in the sampled data, it is required to validate the variograms of the obtained realizations by comparing them with the variogram of the original samples of iron grade. According to Figures 16 and 17, the variograms of the SGCS for both grid sizes of 5x5x1 m and 10x10x1 m are compared with the original variogram of iron grade, which can be additionally observed in Figure 14. SGCS realizations for both of the grid resolutions - 5x5x1 m and 10x10x1 m - reproduced variograms and showed a string match with the experimental variograms, which indicates that the simulations successfully captured the spatial variability and anisotropy of the iron grade distribution across the Haveri tailings facility.

By preserving the correlation structure, SGCS contributes to more realistic spatial modeling, offering valuable insights into ore distribution and variability. The success of variogram reproduction in this study validates the reliability of the SGCS approach and highlights the importance of careful variogram modeling when working with non-additive variables. It also demonstrates the effectiveness of block support in maintaining spatial relationships over larger estimation units, contributing to more robust and geologically coherent resource models.

# 6. CONCLUSIONS AND RECOMMENDATIONS

This study successfully developed the geological model of non-additive iron grade within the Haveri tailings storage facility using Sequential Gaussian Co-Simulation (SGCS) integrating a block-support system. To conduct the SGCS technique, normalized density as a secondary variable and Fe*density as an additive proxy were implemented. The outcomes partially preserved the statistical parameters of Fe grade. The Iron grade simulation over 10x10x1 m grid demonstrated stronger smoothing effect, while maintaining broader trends. The 5x5x1 m grid simulation for Iron grade, provided better results in preserving variance, with enhanced reproducing histograms, and capturing local heterogeneities. The replication of variogram, swath plot, and histogram analyses confirmed the method's ability to replicate the statistical and geographical characteristics of the observed data. Nonetheless, block averaging's induced smoothing effect a limitation for both grids. To improve the preservation of fine-scale variability, future developments should focus on using post-simulation approaches as histogram matching or local variance changes. While also pointing areas for improvement, the proposed SGCS method successfully addressed the difficulties of modeling non-additive components in a heterogeneous tailings environment.

**Key Findings**

- **Non-Additive Variables:** Iron grade, a non-additive variable, presented modeling challenges when using traditional kriging methods. SGCS addressed this limitation by enabling the simulation of spatially distributed Fe grades without relying on linear averaging, thus preserving distribution characteristics and spatial continuity.
- **Block Support Advantage:** The application of block support was effective in mitigating the impact of small-scale noise and facilitating estimation at an operationally meaningful scale. The 5x5x1 m and 10x10x1 m block sizes enabled the comparison of scale-dependent behavior. The 5x5x1 m grid maintained a better balance between detail and smoothing, while the 10x10x1 m grid emphasized larger-scale trends but with more pronounced smoothing effects.
- **Validation Techniques:** Histograms confirmed good reproduction of statistical parameters, though smoothing reduced extreme value representation. Swath plots showed that spatial trends were preserved across the grid, particularly in horizontal directions. Variogram reproduction validated the modeling of spatial structure and

anisotropy, confirming the robustness of the SGCS approach (Goovaerts, 1997; Rossi & Deutsch, 2014).

**Recommendations**

1. **Improved Secondary Variable Estimation**

   The success of SGCS depends heavily on the accuracy of the secondary variable used in co-simulation. In this study, density was used based on a limited number of samples. To improve reliability, future studies should prioritize direct measurement of density or use more robust estimation techniques, such as combining dry density with porosity estimations as proposed by Blannin et al. (2023).

2. **Advanced Data Transformation Techniques**

   To better handle non-linear or complex relationships between variables, future studies could adopt stepwise conditional transformation or principal component-based approaches (Leuangthong & Deutsch, 2003). These methods are particularly useful when cross-plots reveal non-linear dependencies and when dealing with multiple secondary variables.

3. **Increase Sampling in Vertical Direction**

   The study observed greater deviation in vertical swath plots due to low sampling along depth. Future tailings characterization campaigns should improve borehole coverage, particularly in the vertical axis, to support better variogram modeling and vertical continuity assessment.

Overall, the SGCS with block support has proven to be a powerful and flexible tool for modeling non-additive variables in geologically complex environments like TSFs. The insights obtained in this study can be applied to other mining and environmental contexts, particularly where data limitations and heterogeneity pose challenges.

# 7. REFERENCES


Abildin, A., Madani, N., & Topal, E. (2018). Geostatistical modelling of geometallurgical variables through turning bands approach. *25th World Mining Congress 2018: Proceedings Geological Exploration*, 6–16.

Adeli, A., Dowd, P. A., Emery, X., & Xu, C. (2021). Using cokriging to predict metal recovery accounting for non-additivity and preferential sampling designs. *Minerals Engineering*, *170*, Article 106923. https://doi.org/10.1016/j.mineng.2021.106923

Afeni, T. B., Akeju, V. O., & Aladejare, A. E. (2021). Assessment of geological uncertainty through geostatistical simulation: A case study of Itakpe Iron Ore Deposit. *Journal of Mining and Geology*, *57*(1), 91–102.

Almeida, A. S., & Journel, A. G. (1994). Joint simulation of multiple variables: A Markov-type approach. *Mathematical Geology*, *26*(5), 565–588. https://doi.org/10.1007/BF02089242

Babak, O., & Deutsch, C. V. (2009). Statistical approach to inverse distance weighting. *Stochastic Environmental Research and Risk Assessment*, *23*, 543–553. https://doi.org/10.1007/s00477-008-0226-6

Bai, T., & Tahmasebi, P. (2022). Sequential Gaussian simulation for geosystems modeling: A machine learning approach. *Geoscience Frontiers*, *13*(1), Article 101258. https://doi.org/10.1016/j.gsf.2021.101258

Bamigboye, G. O., Bassey, D. E., Olukanni, D. O., Ngene, B. U., Adegoke, D., Odetoyan, A. O., Kareem, M. A., Enabulele, D. O., & Nworgu, A. T. (2021). Waste materials in highway applications: Generation and utilization implications on sustainability. *Journal of Cleaner Production*, *283*, Article 124581. https://doi.org/10.1016/j.jclepro.2020.124581

Blannin, R., Frenzel, M., Tolosana-Delgado, R., Büttner, P., & Gutzmer, J. (2023). 3D geostatistical modelling of a tailings storage facility: Resource potential and environmental implications. *Ore Geology Reviews*, *154*, Article 105337. https://doi.org/10.1016/j.oregeorev.2023.105337

Boisvert, J. B., Rossi, M. E., & Deutsch, C. V. (2009). Multivariate geostatistical simulation of proportions and non-additive geometallurgical variables. *Centre for Computational Geostatistics Annual Report, 11*, Paper 303.

Boucher, A., & Dimitrakopoulos, R. (2012). Multivariate block-support simulation of the Yandi iron ore deposit, Western Australia. *Mathematical Geosciences*, *44*(4), 449–468. https://doi.org/10.1007/s11004-012-9397-y

Brindha, K., Semiromi, M. T., Boumaiza, L., & Mukherjee, S. (2023). Comparing deterministic and stochastic methods in geospatial analysis of groundwater fluoride concentration. *Water*, *15*(9), Article 1707. https://doi.org/10.3390/w15091707

Carrasco, P., Chiles, J. P., & Seguret, M. (2008). Additivity and block support in geostatistics: Implications for grade estimation and control. *Mathematical Geosciences*, *40*(6), 615–633. https://doi.org/10.1007/s11004-008-9167-6

Chen, H. (2022). Techniques of fine reservoir description. In H. Chen (Ed.), *Fine reservoir description* (pp. 113–348). Gulf Professional Publishing.

Emery, X., & Ortiz, J. M. (2011). Cokriging random fields with means related by known linear combinations. *Computers & Geosciences*, *37*(4), 531–544. https://doi.org/10.1016/j.cageo.2010.10.010

European Commission. (2020). Study on the EU's list of critical raw materials (2020): Final report. Publications Office of the European Union. https://doi.org/10.2873/11619

Garrido, M., Ortiz, J. M., Villaseca, F., Kracht, W., Townley, B., & Miranda, R. (2019). Change of support using non-additive variables with Gibbs Sampler: Application to metallurgical recovery of sulphide ores. Computers & Geosciences, 122, 68–76. https://doi.org/10.1016/j.cageo.2018.10.002

Goovaerts, P. (1997). *Geostatistics for natural resources evaluation.* Oxford University Press.

Goovaerts, P. (2016). Sample support. In *Wiley StatsRef: Statistics Reference Online*. https://doi.org/10.1002/9781118445112.stat07754.pub2

Guastaldi, E. (2011). Geostatistical modeling of uncertainty for the risk analysis of a contaminated site. *Journal of Water Resource and Protection, 3*(8), 563–583. https://doi.org/10.4236/jwarp.2011.38066

Herrington, R. (2021). Mining our green future. *Nature Reviews Materials, 6*, 456–458. https://doi.org/10.1038/s41578-021-00325-9

Khalil, A., Koucham, M., & El-Adnani, M. (2023). 3D Geostatistical modeling and metallurgical investigation of Cu in tailings deposit. *Minerals, 14*(893). https://doi.org/10.3390/min14090893

Koucham, M., Benzaazoua, M., & Plante, B. (2024). Reprocessing tailings: A sustainable strategy for extracting critical raw materials. *Resources Policy, 87*, Article 104260. https://doi.org/10.1016/j.resourpol.2024.104260

Leal, R. S., Peroni, R. L., Costa, J. F. C. L., Pereira, S. G., Martins, R. M., & Capponi, L. N. (2016). Geostatistics applied to geometallurgical modeling. In 24th World Mining Congress: Mining in a World of Innovation (pp. 1–8). Rio de Janeiro, Brazil.

Leuangthong, O., & Deutsch, C. V. (2003). Stepwise conditional transformation for simulation of multiple variables. *Mathematical Geology, 35*(2), 155–173. https://doi.org/10.1023/A:1023230907804

Madani, N., Yagiz, S., & Adoko, A. C. (2018). Spatial mapping of the rock quality designation using multi-Gaussian kriging method. Minerals, 8(11), 530. https://doi.org/10.3390/min8110530

Mourlanette, P., Biver, P., Renard, P., Nœtinger, B., Caumon, G., & Perrier, Y. A. (2020). Direct simulation of non-additive properties on unstructured grids. *Advances in Water Resources, 143*, Article 103665. https://doi.org/10.1016/j.advwatres.2020.103665

Parviainen, A., Soto, F., & Caraballo Monge, M. A. (2020). Revalorization of Haveri Au-Cu mine tailings (SW Finland) for potential reprocessing. *Journal of Geochemical Exploration, 218*, Article 106614. https://doi.org/10.1016/j.gexplo.2020.106614

Rossi, M. E., & Deutsch, C. V. (2014). *Mineral resource estimation.* Springer. https://doi.org/10.1007/978-1-4020-5717-5

Shademan, M., & Farhadian, H. (2023). Contribution of geostatistical modeling on simulating a geomechanical parameter (case study: Gol-Gohar open pit iron mine). *Journal of Geomine, 1*(2), 81–91. https://doi.org/10.22077/jgm.2023.6696.1013

Webster, R., & Oliver, M. A. (2007). *Geostatistics for environmental scientists* (2nd ed.). John Wiley & Sons. https://doi.org/10.1002/9780470517277

Zhexenbayeva, A., Madani, N., Renard, P., & Straubhaar, J. (2024). Using multiple-point geostatistics for geomodeling of a vein-type gold deposit. Applied Computing and Geosciences, 23, 100177. https://doi.org/10.1016/j.acags.2024.100177